



Rise over Thermal Estimation Algorithm Optimization and Implementation

Saba Irshad
Purna Chandra Nepal

This thesis is presented as part of Degree of
Master of Science in Electrical Engineering

Blekinge Institute of Technology
February 2013

Blekinge Institute of Technology
School of Engineering
Department of Electrical Engineering
Supervisor: Michael Holmgren M
Examiner: Sven Johansson

Abstract

The uplink load for the scheduling of Enhanced-Uplink (E-UL) channels determine the achievable data rate for Wideband Code Division Multiple Access (WCDMA) systems, therefore its accurate measurement carries a prime significance. The uplink load also known as Rise-over-Thermal (RoT), which is the quotient of the Received Total Wideband Power (RTWP) and the Thermal Noise Power floor. It is a major parameter which is calculated at each Transmission Time Interval (TTI) for maintaining cell coverage and stability. The RoT algorithm for evaluation of uplink load is considered as a complex and resource demanding among several Radio Resource Management (RRM) algorithms running in a radio system. The main focus of this thesis is to study RoT algorithm presently deployed in radio units and its possible optimization by reducing complexity of the algorithm in terms of memory usage and processing power.

The calculation of RoT comprises three main blocks a Kalman filter, a noise floor estimator and the RoT computation. After analyzing the complexity of each block it has been established that the noise floor estimator block is consuming most of the processing power producing peak processor load since it involves many complex floating point calculations. However, the other blocks do not affect the processing load significantly. It was also observed that some block updates can be reduced in order to decrease the average load on the processor.

Three techniques are proposed for reducing the complexity of the RoT algorithm, two for the reduction of peak load and one for the reduction of average load. For reducing the peak load, an interpolation approach is used instead of performing transcendental mathematical calculations. Also, the calculations involving noise floor estimation are extended over several TTIs by keeping in view that the estimation is not time critical. For the reduction of average load, the update rate for the Kalman Filter block is reduced. Based on these optimization steps, a modified algorithm for RoT computation with reduced complexity is proposed. The proposed changes are tested by means of MATLAB simulations demonstrating the improved performance with consistency in the output results. Finally, an arithmetic operation count is done using the hardware manual of Power PC (PPC405) used in Platform 4, which gives a rough estimate of decrease in the percentage of calculations after optimization.

Keywords: Enhanced Uplink (E-UL), Rise-over-Thermal (RoT), Thermal noise power floor, Uplink load, scheduling

Table of Contents

CHAPTER ONE	8
1 INTRODUCTION.....	8
1.1 MOTIVATION.....	9
1.2 OBJECTIVES.....	10
1.3 WAY OF WORK (WoW).....	11
1.4 THESIS ORGANIZATION	11
CHAPTER TWO	13
2 WCDMA IN THIRD GENERATION SYSTEMS.....	13
2.1 Overall Architecture.....	13
2.2 POWER CONTROL	14
2.3 SOFTER AND SOFT HANDOVERS	16
2.4 WCDMA EVOLUTION.....	17
2.4.1 High-Speed Downlink Packet Access.....	18
2.4.2 Enhanced Uplink	19
CHAPTER THREE.....	21
3 RISE OVER THERMAL ESTIMATION CONSTRAINTS	21
3.1 RISE OVER THERMAL.....	21
3.2 PROBLEMS ASSOCIATED WITH LOAD ESTIMATION	22
3.2.1 Effect of Reference and Measurement Points	23
3.2.2 Problems associated with noise floor estimation.....	23
3.3 SOLUTIONS FOR LOAD ESTIMATION	32
3.3.1 Solution for scale factor errors.....	32
3.3.2 Solution for noise floor estimation.....	32
3.4 SUMMARY	32
CHAPTER FOUR.....	33
4 DETAILED DESCRIPTION OF THE CURRENT ALGORITHM	33
4.1 INTRODUCTION.....	33
4.2 BLOCK DIAGRAM OF ROT	34
4.2.1 ALGORITHM BLOCK 0 – RTWP LEVEL ADJUSTMENT	34
4.2.2 ALGORITHM BLOCK 1 – KALMAN FILTER	36
4.2.3 ALGORITHM BLOCK 2 – PRIOR HISTOGRAM.....	39
4.2.4 ALGORITHM BLOCK 3 – SOFT NOISE FLOOR ESTIMATOR	40
4.2.5 ALGORITHM BLOCK 4 – R _{oT} COMPUTATION	44
4.2.6 ALGORITHM BLOCK 5 – BRANCH SUMMATION.....	44
CHAPTER FIVE.....	45
5 PROPOSED OPTIMIZED SOLUTION OF THE ALGORITHM.....	45
5.1 BLOCKWISE ANALYSIS OF THE CURRENT ALGORITHM.....	45
5.1.1 Kalman Filter – Block 1.....	45
5.1.2 Noise Floor Estimator – Block 3	46
5.2 PROPOSED SOLUTION FOR OPTIMIZATION	47
5.2.1 Methods to Reduce Processor Load.....	48
5.3 SUMMARY	55
CHAPTER SIX.....	56
6 CONCLUSIONS AND FURTHER WORK.....	56

Table of figures

FIGURE 1.1 WCDMA AND GSM CORE NETWORK INFRASTRUCTURE	9
FIGURE 1.2 RISE-OVER-THERMAL	10
FIGURE 1.3 SCRUM TASK BOARD	11
FIGURE 2.1 UMTS NETWORK.....	14
FIGURE 2.2 POWER CONTROL.....	15
FIGURE 2.3 SOFTER HANDOVER.....	16
FIGURE 2.4 SOFT HANDOVER.....	17
FIGURE 2.5 ENHANCED UPLINK SCHEDULING FRAMEWORK	20
FIGURE 3.1 AN ILLUSTRATION OF RECEIVED TOTAL WIDEBAND POWER MEASURED AT THE RBS.....	22
FIGURE 3.2 SIGNAL CHAIN ASSUMED FOR LOAD ESTIMATION.....	23
FIGURE 4.1 ROT BLOCK DIAGRAM	34
FIGURE 4.2 FLOW CHART - LEVEL ADJUSTMENT ALGORITHM	36
FIGURE 4.3 KALMAN FILTER.....	39
FIGURE 4.4 PRIOR BLOCK.....	40
FIGURE 4.5 NOISE FLOOR ESTIMATOR	40
FIGURE 4.6 ROT COMPUTATION BLOCK	44
FIGURE 5.1 PROPOSED BLOCK DIAGRAM.....	48
FIGURE 5.2 ROT (WITHOUT TABULATION).....	50
FIGURE 5.3 ROT (WITH TABULATION)	51
FIGURE 5.4 CALCULATIONS INVOLVED IN NOISE FLOOR ESTIMATION.....	51
FIGURE 5.5 UPDATE OF NOISE FLOOR IN 4 TTIS.....	53
FIGURE 5.6 RTWP FROM BLOCK 0 AND BLOCK 1 (KALMAN FILTER)	54
FIGURE 5.7 UPDATE RATE OF KALMAN FILTER.....	55

CHAPTER ONE

1 INTRODUCTION

In today's world the research in communication is evolving, developing and expanding day by day. With an everyday increase in the number of users everyday, the cellular network is expanding, resulting in the requirement of more resources but at the same time keeping the reliability and efficiency at a remarkable level. Wideband Code Division Multiple Access-WCDMA is the world's leading 3G technology that provides high-speed data and voice communication services [1]. It was developed in order to create a global standard for real time multimedia services. In 2000, the standardization of GSM was moved from the European Telecommunications Standards Institute (ETSI) to the Third Generation Partnership Project (3GPP). The 3GPP 1999 standard was focused on data transmission flexibility while maintaining compatibility with previous generation resources. With 3GPP Release 5 the standard incorporated High Speed Downlink Packet Access (HSDPA) featuring shared channel transmission, adaptive modulation, shorter transmission time interval (TTI) and a data rate up to 14.4 Mbps. In addition to existing Quadrature Phase Shift Keying (QPSK), modulation scheme is enhanced to incorporate 16QAM (Quadrature Amplitude Modulation) for higher data rates. 3GPP Release 6, focused on the improvement of the uplink channel through the implementation of High Speed Uplink Packet Access (HSUPA), also known as Enhanced Uplink (EUL) [1], providing a data rate up to 5.76 Mbps. The purpose of the EUL is to improve the performance of uplink dedicated transport channels, i.e. to increase capacity, throughput and reduce delay. HSUPA uses a packet scheduler, but it operates on a request-grant principle where the User Equipments (UEs) request a permission to send data and the scheduler decides when and how many UEs will be allowed to do so. A variety of new channels named E-DCH (Enhanced Dedicated Channel), E-DPDCH (Enhanced Dedicated Physical Data Channel), and E-DPCCH (Enhanced Dedicated Physical Control Channel) have been introduced for HSUPA to enable the system to carry the high speed data. It is extremely necessary to keep a track of progress in technology in a way to make it more efficient in terms of the utilization of resources.

WCDMA is a development from GSM and CDMA. The network structure is based on GSM and the air interface on CDMA. It consists of the Core Network, the Radio Access Network and the Service Network. The GSM Base Station Subsystem (BSS) and the WCDMA Radio Access Network (RAN) are both connected to the GSM core network as can be seen in figure 1.1, providing a radio connection to UE facilitating the two technologies to use the same core network. The core network comprises of the Base Station Subsystem (BSS) and Radio Network controller (RNC) in case of GSM and WCDMA respectively. Both BSS and RNC are connected to the Mobile Switching Center MSC through Media Gateway (MGW). The MGW is further connected to Public Switched Telephone Network (PSTN), Mobile Packet Backbone Network (M-PBN) through Service GPRS Support Node (S-GSN), Intranet and Internet through Gateway GPRS Support Node (G-GSN).

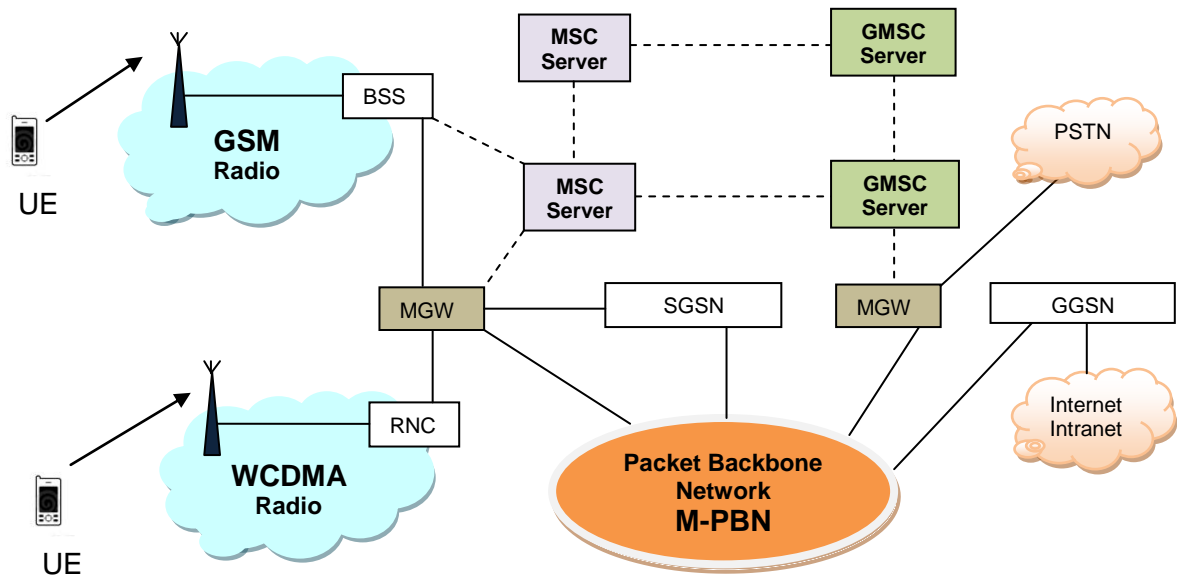


Figure 1.1 WCDMA and GSM Core Network infrastructure

1.1 MOTIVATION

A technical challenge in the WCDMA systems is the scheduling of EUL channels to time intervals where the interference conditions are favorable. The users within the cell and terminals in the neighbor cells contribute to the interference level in the uplink of WCDMA systems. The load of the cell is directly related to the interference level of the same cell; therefore, load should be kept below a certain level to keep the stability of a cell. All cellular radio systems have radio resource management (RRM) algorithms which rely on some sort of resource quantity [2]. These algorithms keep the power of the received signal of each channel at a certain signal to interference ratio (SIR). This SIR level is such that the received powers at the radio base station (RBS) are several dBs below the interference level. Keeping that in view a single user entering the same cell can raise the interference level thereby temporarily reducing the SIR for other users which results in an increase in power by the RBS to all other users thereby increasing the interference more. This can lead to instability and an increase in power rush. Therefore it is extremely important to schedule high capacity uplink channels, like EUL channel in WCDMA to avoid the instability caused by the reason mentioned above.

The load in a cell is typically related to power, that is, noise rise. Out of a number of noise rise parameters the most important is Rise over Thermal (RoT) which is defined as the quotient between total interference in the cell, received total wideband power (RTWP) at the RBS and the thermal noise power floor as depicted in the following equation 1.1. Therefore, it is extremely important to measure the noise floor accurately.

Equation 1.1

$$RoT = \frac{RTWP}{ThermalNoisePowerFloor}$$

The received power level and the thermal power floor vary with time. To ensure the planned coverage and cell stability uplink load must be with the certain range which is defined as the RoT limit as shown the figure 1.2

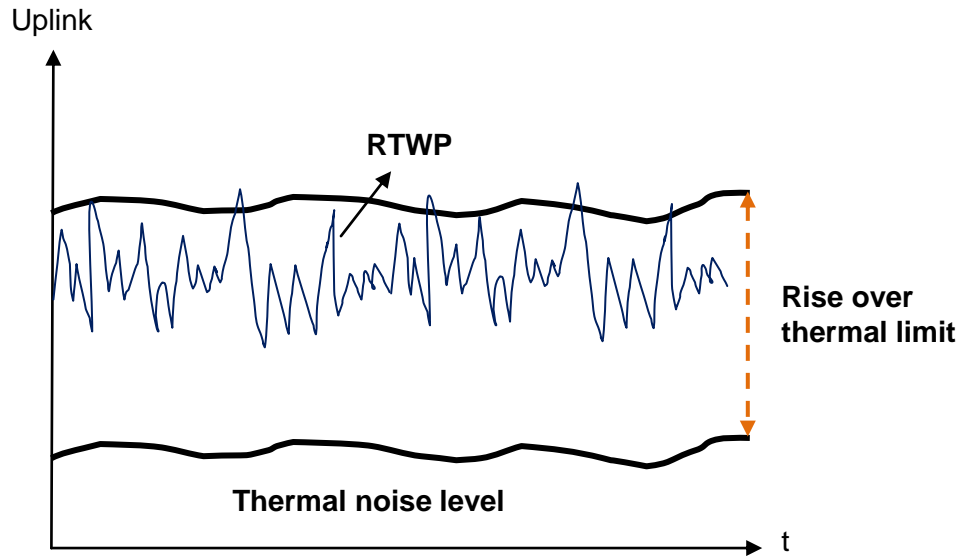


Figure 1.2 Rise-over-Thermal

Radio Units contain numerous signal processing algorithms running in a real time environment. As Radios get more and more digital it is important to optimize the implemented algorithms with respect to code size, data memory usage, processing speed and energy consumption. Uplink load of a cell is an important quantity which must be estimated in order to schedule the uplink users to the time intervals where the interference is minimum. Out of several algorithms running in the radio, RoT, for the estimation of load is perhaps the most resource demanding algorithm which consumes about 60-70% of the processor load and in worse conditions it could raise as high as up to 100%. With increasing traffic everyday, it is extremely important to optimize the algorithm and its implementation for efficient optimal utilization of radio resources.

1.2 OBJECTIVES

With the aforementioned, the objectives of this thesis are as follows:

- To study and understand the current algorithm in detail in order to investigate the possible ways to optimize it in terms of processing power and memory usage.
- Modifications in the current algorithm required for optimization, simulation in MATLAB and implementing the algorithm in C++
- Verification of the optimized algorithm, to prove that it is working as expected and more efficient compared to the previous one without any performance loss.

1.3 WAY OF WORK (WoW)

During the thesis duration scrum with two week sprint have been followed figure 1.3. Planning meeting within the team was carried out at the beginning of each sprint followed with weekly follow up meeting and demonstration by the end of sprint. Several meeting with experts were carried out during the entire period. Discussions during the meeting were quite helpful carrying out the research work. The research work was successfully completed in 24 weeks.



Figure 1.3 Scrum Task board

1.4 THESIS ORGANIZATION

The thesis is organized in six chapters; each of them starts with an introduction and ends with a short summary.

Chapter 1 comprises of a short introduction, the problem statement, motivation behind the thesis, thesis objectives and the contribution of the thesis.

Chapter 2 addresses the basic background about WCDMA and the channels, which strengthen the base of the body of the thesis in the coming chapters.

Chapter 3 starts with the explanation of actual topic of the thesis, general aspects of RoT estimation, the constraints associated with the measurement of RoT, and a detailed description of the terms and parameters that will be used in the coming chapters.

Chapter 4 gives a comprehensive view of the implemented algorithm for the computation of RoT. It explains each and every step in detail towards the final result.

Chapter 5 is in continuation of the former chapter, which will explain the proposed changes in the current algorithm in order to optimize it. It will also give an analysis after the proposed changes.

Chapter 6 ends the thesis with conclusions drawn from this work and future work that could be done to avoid the unnecessary processor load in the Radio Unit.

CHAPTER TWO

2 WCDMA IN THIRD GENERATION SYSTEMS

During the past years, there has been a quickly rising interest in radio access technologies for mobile and fixed service for voice, video and data. Third Generation technology was introduced which features increased bandwidth and data transfer rates to accommodate Web based applications and phone based audio and video [3]. Wideband Code Division Multiple Access (WCDMA) technology has emerged as the most widely adopted third generation air interface [1]. Its specification has been created in 3GPP (the 3rd Generation Partnership project), which is a joint standardization project of the standardization bodies from Europe, Japan, Korea, USA and China. WCDMA is called UTRA (Universal Terrestrial Radio Access), FDD (Frequency Division Duplex) [4] and TDD (Time Division Duplex), within 3GPP; both FDD and TDD operation are covered by the name WCDMA.

WCDMA provides simultaneous support for a wide range of services with different characteristics on a common 5 MHz carrier [1]. WCDMA supporting both high rate packet data and circuit switched services are designed to be service independent, in order to accommodate a flexible introduction of new services and a mixture of services.

2.1 Overall Architecture

The Universal Mobile Telecommunications System (UMTS) [5] network consists of three interacting domains: Core Network (CN), UMTS Terrestrial Radio Access Network (UTRAN) and User Equipment (UE) [6] as illustrated in Figure 2.1. The UE with USIM (Universal SIM) communicates with one or several NodeBs. NodeB refers to a logical node, responsible for physical layer processing such as physical channel coding, modulation/demodulation, closed loop power control, error handling etc. USIM contains member specific data and enables the authenticated entry of the subscriber into the network. The Radio Network Controller (RNC) [5] controls multiple NodeBs; major functions of the RNC are radio resource management, power control, channel allocation, admission control, segmentation/reassembly etc.

The main function of Core Network (CN) is to provide switching, routing and transit for user traffic also contains the databases and network management functions. The CN is divided into two domains CS (Circuit Switched) and PS (Packet Switched) domains [6]. Circuit switched elements are the Mobile Services Switching Centre (MSC), Visitor Location Register (VLR) and Gateway MSC. Packet switched elements are the Serving GPRS Support Node (SGSN) and the Gateway GPRS Support Node (GGSN), the network elements like HLR, EIR and AUC are shared by both domains.

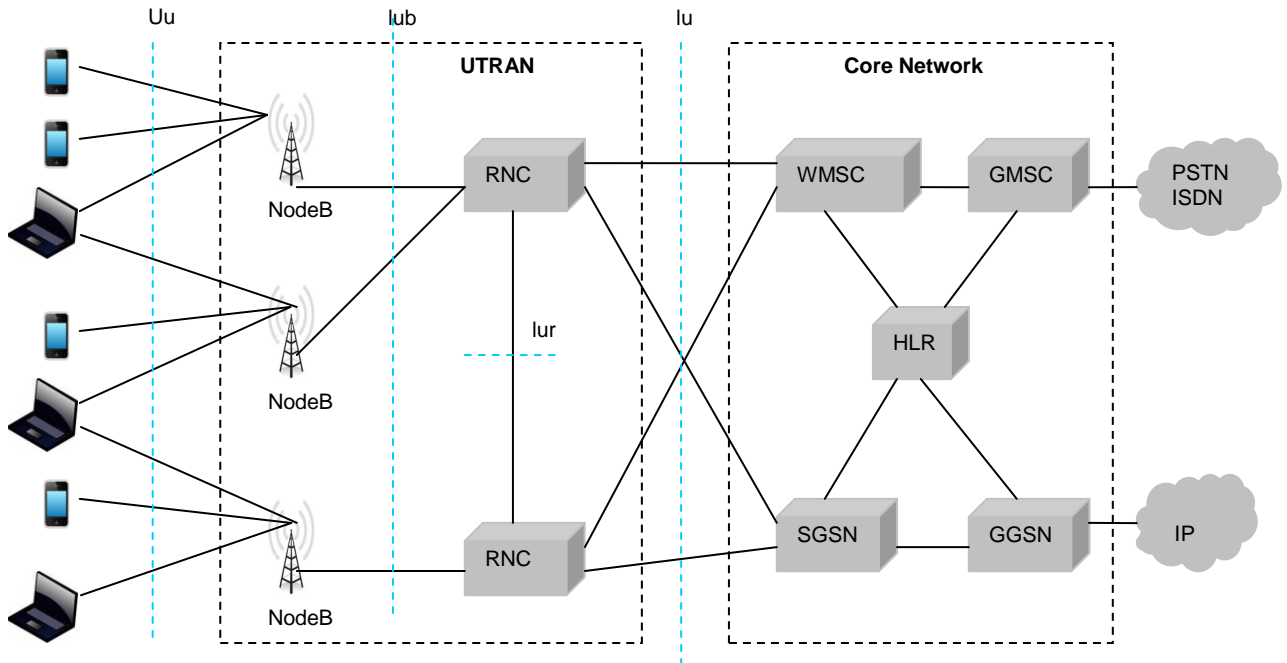


Figure 2.1 UMTS Network

2.2 POWER CONTROL

One of the most important requirements in the WCDMA system is the capability of the user equipment (UE) and base transceiver stations to control their transmitter power output [1]. Without this capacity, the system will not work effectively and attain its full capacity and also a single overpowered mobile could block a whole cell. Figure 2.2 depicts the far near problem and the solution in the form of closed loop transmission power control.

User equipments UE1 and UE2 operate within the same frequency, separable at the base station only by their respective spreading codes [1]. Base station is receiving signals simultaneously from two mobile stations, one close to the base station and the other near the edge of a cell. Because UE1 is closer than UE2, if both mobile stations are transmitting at the same level, the signal from UE1 will be stronger than the signal from UE2. As the received SIR for UE2 is lower, the detection of the signal at the base station is subject to a higher bit error rate. Depending upon the relative distances d_1 and d_2 , the stronger signal may swamp out the weaker signal [6]. Furthermore, the two signals fade independently; it is possible that the instantaneous value of the signal from UE1 is above its average level while at the same time the signal from UE2 is substantially below its mean, thus making it more difficult for the base station to detect the weaker signal.

To overcome this problem, the base station measures the signal from a mobile station, depending upon the signal level relative to a threshold, it sends a command to increase or decrease its power level to that station, so that the signal that the base station receives from that mobile station is equal to signals from the other mobile stations. Another benefit of the power control is that mobile stations may now be able to operate at an optimal power level. Thus, WCDMA handsets may have more compact design and longer battery life. It would also result in improved speech quality, in urban and dense urban areas. System capacity (the maximum number of mobile stations that can be served in a system) is maximum when the transmitter power of each mobile station is adjusted such that the received SIR from each mobile is just about enough to maintain the desired quality.

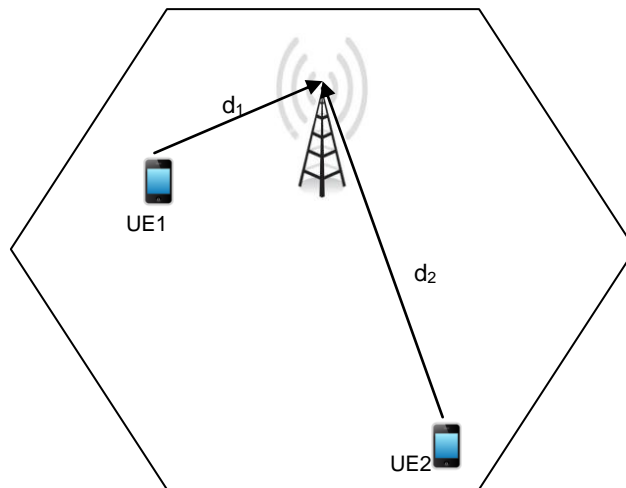


Figure 2.2 Power Control

To insure the base station receives a satisfactory SIR from each mobile, power control [7] is applied on an uplink channel [8]. The base station measures the received signal strength, and if it is outside the limits of satisfactory operation, it orders the mobile station to adjust its transmit power accordingly.

As it is based upon direct measurement of the desired signal, this is called a closed loop power control. Next approach, we could control the transmitter power on an uplink channel by measuring a different parameter that only gives an indirect indication of the transmitter power. For example, the mobile station could measure the signal received from the base station, estimate the path loss on the forward channel, and accordingly adjust the transmit power of the reverse channel. Clearly, this adjustment works only if the path loss variations on the forward and reverse channels are correlated [7]. This is known as open loop power control. Thus, we can use both open and closed loop controls on a reverse channel. Power control is also used on downlink channel to insure each mobile station receives a satisfactory signal level from the base station. Here, the algorithm are usually closed loop where each mobile station measure the received signal on the forward channel and, based upon the measurements, requests the base station to adjust its transmit power.

2.3 SOFTER AND SOFT HANDOVERS

When a mobile station moves from the serving area of one base station to the serving area of a second, the signal received from this station is stronger so it should eventually communicate with the second base station. This process of switching communication from one base station to another is called a handover. There are different types of handoffs in WCDMA system.

A mobile station is in the overlapping cell coverage area of two adjacent sectors of a base station during softer handover. Mobile station communicates with base station concurrently via two air interface channels, one of each sector separately [5]. This requires the use of two separate codes in the downlink direction, so that the mobile station can distinguish the signals. Figure 2.3 shows the softer handover scenario.

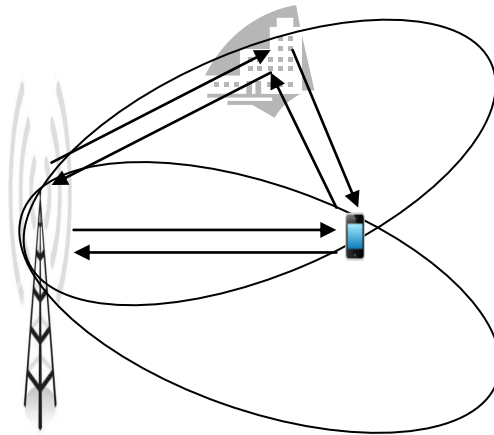


Figure 2.3 Softer Handover

During soft handover figure 2.4, a mobile station is in the overlapping cell coverage area of two sectors belonging to different base stations. Similarly, the communications between mobile station and base station take place concurrently via two air interface channels for each base station separately [5].

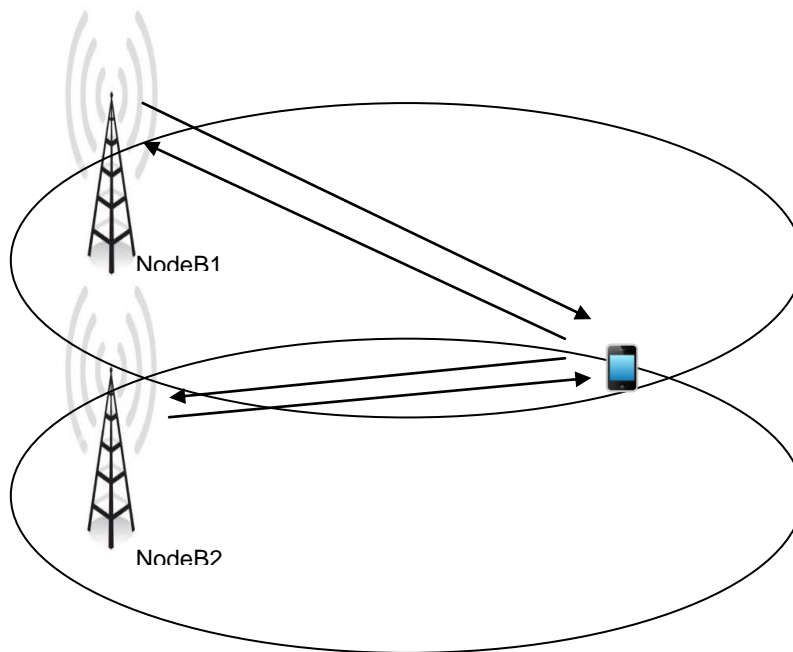


Figure 2.4 Soft Handover

In addition to soft/softer handover, WCDMA provides other handover types as well [6]:

- Inter-frequency hard handovers that can be used to hand a mobile over from one WCDMA frequency carrier to another. This is applicable for the high capacity base stations with several carriers.
- Inter-system hard handover that take place between the WCDMA FDD system and another system, such as WCDMA TDD or GSM.

2.4 WCDMA EVOLUTION

Introduction of High Speed Downlink Packet Access (HSDPA) is the first step in the evolution of WCDMA radio access in Release 5 of the 3GPP/WCDMA specifications [4]. HSDPA brings further enhancements to the already supported packet data communication in the first release, both in terms of system and end-user performance. Enhanced Uplink, introduced in Release 6 of the 3GPP/WCDMA specification complements the downlink packet-data enhancement of HSDPA [4]. HSDPA and Enhanced Uplink are often jointly referred to as High Speed Packet Access (HSPA). High data rates and low delays are the important requirements for cellular systems providing packet-data services at the same time, maintaining good coverage and providing high capacity. HSPA introduces several of the basic techniques into WCDMA, such as higher order modulation, fast (channel-dependent) scheduling and rate control, and fast hybrid ARQ with soft combining.

2.4.1 High-Speed Downlink Packet Access

In WCDMA 3GPP Release 5, HSDPA is designed to support data rates up to 14.4 Mbps over a 5 MHz bandwidth [4]. HSDPA incorporates several attractive features including High speed shared channel transmission (both in code and time domains), Adaptive modulation and coding schemes (AMC), Hybrid Automatic Repeat Request (HARQ), Short transmission time interval (TTI) and fast scheduling.

Five different physical channels and one transport channel is introduced to support HSDPA as shown in the following table:

Channels	Features
Physical Channels	
HS-PDSCH - High Speed Physical Downlink Shared Channel (Downlink)	<ul style="list-style-type: none"> • Spreading Factor (SF) = 16 • QPSK and 16 QAM Modulation • 2ms TTI • No Power Control • No Soft Handover support
HS-SCCH - High Speed Shared Control Channel (Downlink)	<ul style="list-style-type: none"> • QPSK Modulation • Fixed SF = 128 • Support Power Control • No Soft Handover support
HS-DPCCH - High Speed Dedicated Physical Control Channel (Uplink)	<ul style="list-style-type: none"> • Carries Acknowledgment (ACK) • Carries Channel Quality Indication (CQI) • BPSK-Binary Phase Shift Keying • SF=256 • No Soft Handover support
Associated DPCH – Dedicated Physical Channel	<ul style="list-style-type: none"> • Two DPCH one for Uplink (UL) & one for Downlink (DL) • Signaling (DL only) • Data rate 64, 128 or 384 kbps (UL only) • QPSK • SF = 4 to 512 • Soft Handover support (both UL & DL)
Transport Channel	
HS-DSCH High Speed Downlink Shared Channel (Downlink)	<ul style="list-style-type: none"> • Adaptive Modulation • Hybrid Automatic Repeat Request (HARQ)

A key characteristic of HSDPA is the use of Shared-Channel Transmission, which is implemented through the High-Speed Downlink Shared Channel (HS-DSCH). This implies that a certain fraction of the total downlink radio resources available within a cell, channelization codes and transmission power in case of WCDMA, is seen as a common resource that is dynamically shared between users. HS-DSCH enables the possibility to rapidly allocate a large fraction of the downlink resources for transmission of data to a specific user. Shorter TTI is used for HS-DSCH which reduces the overall delay and improves the tracking of fast channel variations exploited by the rate control and the channel-dependent scheduling [1].

The High-Speed Downlink Shared Channel (HS-DSCH) is the transport channel used to support shared-channel transmission and the technologies like channel-dependent scheduling, rate control and hybrid ARQ with soft combining in HSDPA. HS-DSCH corresponds to a set of channelization codes, each with spreading factor 16, which are known as HS-DPSCH High-Speed Physical Downlink Shared Channel.

2.4.2 Enhanced Uplink

Enhanced Uplink [8] provides improvements in WCDMA uplink capabilities and performance in terms of high data rates, reduced latency, and improved system capacity. It has been introduced in WCDMA Release 6, also known as High-Speed Uplink Packet Access (HSUPA). Enhanced Uplink also introduces a short 2 ms uplink TTI and features like fast scheduling and fast hybrid ARQ with soft combining, as for HSUPA [8]. These enhancements are implemented in WCDMA through a new transport channel, the Enhanced Dedicated Channel (E-DCH).

Both HSDPA and Enhanced Uplink uses the same technologies there are some fundamental difference between them, which have affected the detail implementation of the features:

- Shared resources: In the downlink transmission power and the code space, both are located in one central node, the NodeB. In the uplink, it's the amount of allowed uplink interference, which depends on the transmission power of multiple distributed nodes, the UEs.
- In the downlink both the scheduler and the transmission buffer are located in the same node, but in the uplink the scheduler is located in the NodeB while the data buffers are distributed in the UEs.
- In the uplink transmitted channels are non-orthogonal so they are subject to interference between uplink transmissions within the same cell, but in the downlink, transmitted channels are orthogonal.
- Higher order modulation to provide high data rates are possible in the downlink, which trades power efficiency for bandwidth efficiency. But in the uplink higher order modulation is less useful.

2.4.2.1 Scheduling

Scheduling is a key element behind Enhanced Uplink. Scheduler is the only entity responsible for controlling which E-DCH users get what data rate at which time [1]. By increasing the transmission power, the UE can transmit at higher rates, at the same time controlling the amount of interference affecting other users at the NodeB. If the interference level is very high, some transmission in the cell, control channels and the non-scheduled uplink transmissions, may not be received properly and if interference level is too low the full system capacity not used. Hence, EUL relies on the scheduler to give users with high data rate as possible without exceeding the maximum tolerable interference level in the cell.

In HSUPA, the scheduler and transmission buffers both are located in the NodeB; scheduler is responsible to coordinate different UEs transmission activities in the cell. The scheduling decisions are sent to UEs and the buffer information from the UEs is provided to the scheduler [5]. Hence the scheduling framework for EUL is based on scheduling grants sent by the NodeB scheduler to control the UE and scheduling requests sent by the UEs to request resources. With reference to the instantaneous interference level, the scheduler controls the scheduling grant in each terminal to maintain the interference level in the cell. Both inter-cell interference and intra-cell interference should be taken into account by the scheduler for allowing a UE to transmit at a high data rate to insure a stable network operation. The amount of common uplink resources a terminal is using depends on the data rate being used. For the higher data rate, it requires larger transmission power and thus the higher resource consumption.

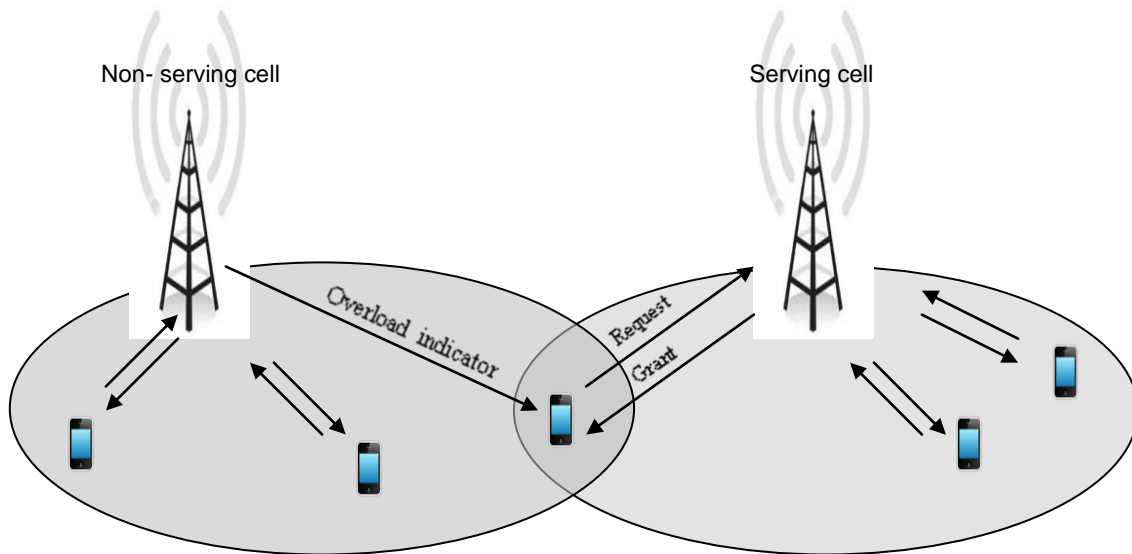


Figure 2.5 Enhanced Uplink scheduling framework

Noise rise or RoT is the ratio between the total uplink power of the cell and the thermal noise floor power [3], which is used for the analyzing uplink operation. It has close relation to coverage and uplink load. It is important for the uplink scheduler to keep the noise rise within the acceptable limits. This concept is further explained in the coming chapters. If noise rise is too large, it would result in loss of coverage for some channels, a terminal may not have sufficient transmission power available to reach the required E_b/N_0 at the base station.

CHAPTER THREE

3 RISE OVER THERMAL ESTIMATION CONSTRAINTS

The purpose of the scheduler and the Uu air interface load estimator is to secure that the uplink interference load is below certain limits. The scheduler can only control the EUL traffic, but the interference can be caused by other sources, both internally in the cell, e.g. DCH-users, and externally generated, e.g. E-DCH-users, DCH-users or the other noise sources. The interference load control has two purposes:

- *Coverage*: to avoid too small uplink coverage due to increased interference level.
- *Stability*: to avoid power rush effects, that happens when the system is close to the pole capacity [5].

The uplink noise increases exponentially with the loading. When the uplink noise approaches infinity then no more users can be added to a cell and the cell loading is close to 100% and has reached its “pole capacity”. Therefore, the accurate estimation of uplink load is extremely important to maintain cell coverage and stability.

In wireless communication systems, the RoT, also known as the uplink load of a cell, indicates the ratio between the total interference received at a base station and the thermal noise [5]. Total interference received, refers to the Received Total Wideband Power (RTWP) which is the sum of inter-cell interference, intra-cell interference and thermal noise power.

The RoT is typically used as a measure of how much a cellular telephone network is congested. The acceptable level of RoT determines the capacity and manages the cell coverage of systems using Code Division Multiple Access (CDMA). This chapter highlights the load estimation constraints, two major problems in the estimation of load and proposes the possible solution to them.

The first part of the chapter focuses on the reference and measurement points; it explains the scale factor errors that are observed at the analogue front end where the power measurements are performed. The second part of the chapter proves that the uplink load is unobservable with any linear estimation technique using measurements (RTWP and Channel powers) in a single Radio Base Station (RBS). This is done by using the state space models with different combinations, showing that only the sum of powers of same cell, the neighbor cell and the noise floor is observable.

Also, it is proved that none of these quantities can be subtracted from the other using mathematical modeling. Later on the principle of load estimation is discussed; chapter ends with some of the advantages of proposed algorithm for the RoT estimation.

3.1 RISE OVER THERMAL

The term Rise-over-Thermal (RoT) also known as uplink load of a cell is defined as:

The quotient of the total uplink power of the cell and the thermal noise power floor

and is given by,

Equation 3.1

$$RoT = \frac{RTWP}{ThermalNoisePowerfloor}$$

The total uplink power RTWP is readily measured on the receiver of the RBS. The RTWP is the sum of uplink WCDMA radio link power of the own cell, uplink WCDMA radio link powers of neighbor cells, any external (non-WCDMA) interference power and thermal noise power. This mechanism is depicted in the figure 3.1.

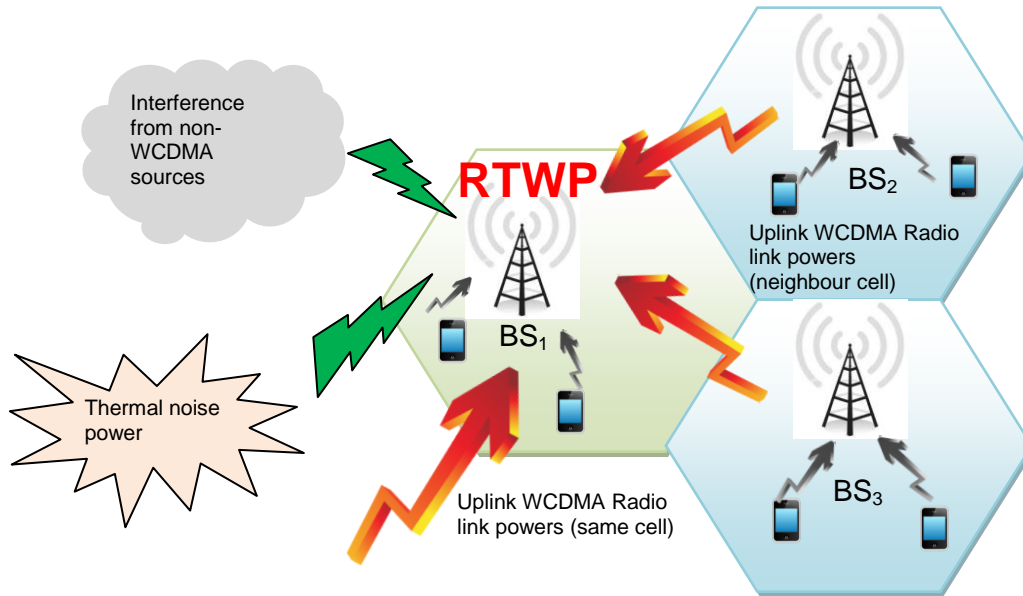


Figure 3.1 An illustration of Received Total Wideband Power measured at the RBS

3.2 PROBLEMS ASSOCIATED WITH LOAD ESTIMATION

One key aspect of the EUL concept as explained in the previous chapter is to add capacity to the system, by scheduling of transmission to time instants where the interference situation is beneficial. One way to avoid the over scheduling of resources is to continuously measure or estimate the load in the cell and base the scheduling on that load estimate. The purpose of the scheduler and the Uu load estimator is to secure that the uplink interference load is below certain limits. The load is to be estimated in terms of noise rise of the cell [5]. The two problems associated with the load estimation are explained below. Section 3.2.1 the over effect of reference and measurement points on received power and the noise floor estimation. Section 3.2.2 explains in detail the problems associated with the noise floor estimation, two approaches to solve these problems are discussed in the sub section of 3.2.2. Both these approaches turn out to be infeasible. Section 3.3 explains the solution to the above mentioned problems.

3.2.1 Effect of Reference and Measurement Points

One of the constraints associated with the load estimation is the selection of reference and measurement points [4]. In a typical signal chain of RBS, a received wideband signal from an antenna first passes an analogue signal conditioning chain (analogue front end) as shown in fig 3.2. This chain consisting of cables, filters etc between the antenna and the digital receiver has scale factor errors of 2-3 dB associated with it. As a result of this the thermal noise floor power as well as the received powers, is affected by the component uncertainties in the analogue receiver front end. The RTWP which is divided by the default value of thermal noise power floor may therefore be inconsistent with the assumed thermal noise power floor by 2-3 dB. The effect would be a noise rise estimate that is also wrong by 2-3 dB. Considering the fact that the allowed noise rise interval in a WCDMA system is 0-7 dB, an error of 2-3 dB is not acceptable.

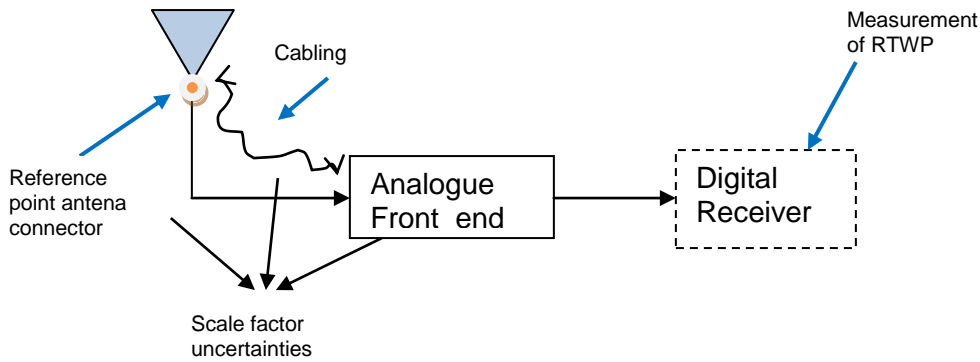


Figure 3.2 Signal Chain assumed for Load estimation

3.2.2 Problems associated with noise floor estimation

Another problem associated with the estimation of noise floor is caused by uncontrollable interferences. The scheduler can only control the EUL traffic, but the interference can be caused by other sources as well, both internally in the cell, externally generated and the other noise sources. As a result of these interferences, the total power measurement (received at the RBS) also contains interference power from neighbor cells and from external sources like airport radars as shown in the figure 3.1 above. These power conditions are indistinguishable from each other and hence none of them can be directly measured, they cannot be estimated by standard estimation techniques. The sought quantity for load estimation is the noise rise, $N_R(t)$ is defined by:

Equation 3.3

$$N_R(t) = \frac{P^{total}(t)}{P_N}$$

The measurements of the RTWP are performed in the receiver. This measurement is denoted by $P^{Total}(t)$, and P_N is the thermal noise power floor level as measured by the antenna connector where t denotes discrete time. The measurement rate is T^{-1} Hz [9]. Mathematically;

Equation 3.4

$$P^{Total}(t) = \sum_{i=1}^N P_i^{Code}(t) + P^{E+N}(t) + P_N$$

Where $P_i^{Code}(t)$ is the sum of control signal power and data channel power for the total channel i , $P^{E+N}(t)$ denotes the power as received from neighbor cells (N) as well as from external sources (E) to the WCDMA system, P_N is the (thermal) noise floor level as measured by the antenna connector. It is clear that unless additional signaling is introduced between RBSs, then $P^{E+N}(t)$ and P_N are not measurable directly and hence they need to be estimated or eliminated in some way.

Two possible approaches to solve the noise floor estimation problem could be:

- Direct estimation of the noise floor, where inter-cell interference is also estimated. Unfortunately the powers are indistinguishable for the estimator, rendering this approach infeasible.
- Use the power control loop to eliminate everything but the thermal noise floor power. This approach also turns out to be infeasible reason being that no matter what power control model is introduced; this model is not capable of controlling neighbor cell uplink powers.

Technically it is proved in section 3.2.2.1 and section 3.2.2.2 that both of the two alternatives mentioned above are infeasible due to the fact that the state vector is not completely observable [10].

3.2.2.1 Linear estimation of $P^{E+N}(t)$ and P_N

a. State space models

The first approach attempts to estimate both $P^{E+N}(t)$ and P_N . Code power measurements are also assumed, in order to (tentatively) enhance performance. The state vector is hence chosen as [13]:

Equation 3.5

$$\mathbf{x}(t) = \begin{pmatrix} P_1^{Code}(t) \\ \vdots \\ P_N^{Code}(t) \\ P^{E+N}(t) \\ P_N(t) \end{pmatrix}$$

With this selection of state vector a linear state space model of the following form can be constructed

Equation 3.6

$$\begin{aligned} \mathbf{x}(t + T_{min}) &= \mathbf{A}(t)\mathbf{x}(t) + \mathbf{B}(t)\mathbf{u}(t) + \mathbf{w}(t) \\ \mathbf{y}(t) &= \mathbf{C}(t)\mathbf{x}(t) + \mathbf{e}(t). \end{aligned}$$

Equation 3.7

$$\mathbf{u}(t) = \begin{pmatrix} P_1^{CodeRef}(t) \\ \vdots \\ P_{n-1}^{CodeRef}(t) \\ P_n^{CodeRef}(t) \end{pmatrix}$$

This results in the conventional linear state space model used for Kalman filter design. Here T_{min} is a smallest sampling period such that all other sampling periods are integer multiples of this sampling period, $\mathbf{u}(t)$ denotes the input signal vector, $\mathbf{y}(t)$ denotes the output signal (or measurement) vector. Furthermore, $\mathbf{A}(t)$ is the system matrix, $\mathbf{B}(t)$ the input gain matrix and $\mathbf{C}(t)$ is the measurement matrix. The vectors $\mathbf{w}(t)$ and $\mathbf{e}(t)$ represent the systems and measurement noise, respectively.

From the equations and alternatives in [9], two pairs of matrices $\mathbf{A}(t)$ and $\mathbf{B}(t)$ can be constructed as:

Equation 3.8

$$\mathbf{A}_1(t) = \begin{pmatrix} 1 & 0 & \dots & 0 \\ 0 & \ddots & & \vdots \\ \vdots & & 1 & \\ & & & 1 & 0 \\ 0 & \dots & & 0 & 1 \end{pmatrix}_{(n+2) \times (n+2)}, \quad \mathbf{B}_1(t) = \begin{pmatrix} 0 \\ \vdots \\ 0 \\ 0 \\ 0 \end{pmatrix}_{(n+2) \times 1}$$

Equation 3.9

$$\mathbf{A}_2(t) = \begin{pmatrix} 1-K & 0 & \dots & 0 \\ 0 & \ddots & & \vdots \\ \vdots & & 1-K & \\ & & & 1 & 0 \\ 0 & \dots & & 0 & 1 \end{pmatrix}_{(n+2) \times (n+2)}, \quad \mathbf{B}_2(t) = \begin{pmatrix} K & \mathbf{0} & 0 \\ 0 & \ddots & \mathbf{0} \\ \vdots & & K \\ & & & 0 \\ 0 & \dots & & 0 \end{pmatrix}_{(n+2) \times n}$$

Where, n is the number of channels and K is the Kalman gain.

In the same way, two measurement matrices $\mathbf{C}(t)$, can be constructed from the alternatives and equations of section 4.2 in [9]

Equation 3.10

$$\mathbf{C}^1(t) = \begin{pmatrix} \frac{1}{1+\eta_1(t)} & 0 & \dots & & 0 \\ 0 & \frac{1}{1+\eta_2(t)} & 0 & \dots & \vdots \\ \vdots & & \ddots & & \\ 0 & & & \frac{1}{1+\eta_n(t)} & 0 & 0 \\ 1 & \dots & & 1 & 1 & 1 \end{pmatrix}_{(n+1) \times (n+2)}$$

Equation 3.11

$$\mathbf{C}^2(t) = \begin{pmatrix} L_1(t) & \dots & L_1(t) \\ \vdots & & \\ L_n(t) & \dots & L_n(t) \\ 1 & \dots & 1 & 1 & 1 \end{pmatrix}_{(n+1) \times (n+2)}$$

Where $\eta(t)$ is the scale factor and it depends on the momentary transport format via the beta factors [10], $L_i(t)$, $i = 1, \dots, n$ denotes the load factors, which represents the relation between a total power and the code reference value for the channel.

All quantities but the system matrix, $\mathbf{A}(t)$ and the measurement matrix, $\mathbf{C}(t)$ are of no consequence for the observability analysis. The input gain matrix, $\mathbf{B}(t)$ is used in the algorithms defined in this section.

b. Observability Analysis

The observability analysis is performed with the following fundamental theorem, found in [11].

Observability Theorem

The unobservable state vectors (of dimension m) are spanned by the null space of the matrix

Equation 3.12

$$\mathbf{O} = \begin{pmatrix} \mathbf{C} \\ \mathbf{CA} \\ \vdots \\ \mathbf{CA}^m \end{pmatrix}$$

This theorem is given for time invariant systems, while there is some slow time variation in the above models. This is less important here, since the unobservable modes are in all cases related to $P^{E+N}(t)$ and P_N , and these quantities have only time invariant blocks related to them. The analysis is therefore performed for the time invariant special case

Using the observability theorem and combining equation 3.8 and equation 3.10, results in:

Equation 3.13

$$\mathbf{C}^1 \mathbf{A}_1 = \begin{pmatrix} \frac{1}{1+\eta_1} & 0 & \dots & & 0 \\ 0 & \frac{1}{1+\eta_2} & 0 & \dots & 0 \\ \vdots & & \ddots & & \vdots \\ 0 & & & \frac{1}{1+\eta_n} & 0 & 0 \\ 1 & \dots & & 1 & 1 & 1 \end{pmatrix} = \mathbf{C}^1 \Rightarrow \mathbf{C}^1 \mathbf{A}^i = \mathbf{C}^1 \quad i = 1, \dots, n+1$$

Hence $rank(\mathbf{O}) = rank\left(\left(\mathbf{C}^1\right)^T \dots \left(\mathbf{C}^1\right)^T\right) = rank(\mathbf{C}^1) \leq n+1 < n+2$ and the system cannot be observable. To determine the unobservable subspace, the following equation is solved (obtained after performing elementary operations to eliminate linearly dependant equations).

Equation 3.14

$$\mathbf{C}^1 \mathbf{x} = \begin{pmatrix} \frac{1}{1+\eta_1} & 0 & \dots & & 0 \\ 0 & \frac{1}{1+\eta_2} & 0 & \dots & 0 \\ \vdots & & \ddots & & \vdots \\ 0 & & & \frac{1}{1+\eta_n} & 0 & 0 \\ 1 & \dots & & 1 & 1 & 1 \end{pmatrix} \begin{pmatrix} P_1^{Code} \\ \vdots \\ P_n^{Code} \\ P^{E+N} \\ P_N \end{pmatrix} = \begin{pmatrix} 0 \\ \vdots \\ 0 \\ 0 \\ 0 \end{pmatrix}$$

This implies

Equation 3.15

$$\begin{pmatrix} P_1^{Code} \\ \vdots \\ P_n^{Code} \\ P^{E+N} \\ P_N \end{pmatrix} = \begin{pmatrix} 0 \\ 0 \\ 0 \\ 1 \\ -1 \end{pmatrix} q$$

where q is an arbitrary parameter. Hence the unobservable subspace is spanned by the vector.

Equation 3.16

$$\begin{pmatrix} 0 \\ \vdots \\ 0 \\ 1 \\ -1 \end{pmatrix}$$

Which clearly shows that only the sum $P^{E+N} + P_N$ is observable from the available measurements. This is perfectly natural since only the sum can be solved for in case code power and total power measurements are available. Since both P^{E+N} and P_N are positive quantities with a nonzero mean, it is not possible to separate the two only from the available measurements.

Note that this situation does not really change for the other three combinations. They are however analyzed formally below to avoid any future concern.

Combining equation 3.10 and equation 3.9 gives us,

Equation 3.17

$$\mathbf{C}^1 \mathbf{A}_2^i = \begin{pmatrix} \frac{(1-K)^i}{1+\eta_1} & 0 & \dots & & 0 \\ 0 & \frac{(1-K)^i}{1+\eta_2} & 0 & \dots & 0 \\ \vdots & & \ddots & & \vdots \\ 0 & & & \frac{(1-K)^i}{1+\eta_n} & 0 & 0 \\ (1-K)^i & \dots & & (1-K)^i & 1 & 1 \end{pmatrix}$$

By subtracting the last column from the second last, it follows again that $\text{rank}(\mathbf{O}) \leq n+1 < n+2$ and the system cannot be observable. A solution to the observability equation:

Equation 3.18 $\mathbf{Ox} = \mathbf{0}$

The above equation can be obtained by using e.g. only the upper block. This renders the solution to equation 3.16. This solution can be verified by insertion in the complete equation and it can again be concluded that only the sum $P^{E+N} + P_N$ is observable from the given measurements.

In this case

Equation 3.19 $\mathbf{C}^2 \mathbf{A}_1^i = \mathbf{C}^2$

Hence this alternative render, by inspection,

$$\text{rank}(\mathbf{O}) = \text{rank}\left(\left(\left(\mathbf{C}^2\right)^T \quad \dots \quad \left(\mathbf{C}^2\right)^T\right)^T\right) = \text{rank}(\mathbf{C}^2) = 1 < n+2$$

where the last step follows from elementary row operations. The combination of the random walk models and the second measurement equation is not a feasible choice. In this case it is not even necessary to solve the observability equation for the null space, it can be concluded immediately that at most one state component can be observed. The reason for this seems to be that the random walk models all have the same dynamics; hence they cannot be independently observed unless they are separately measured and modeled. Note that in case modes with different time constants would appear, the measurement modeling strategy would work.

Combining equation 3.11 and equation 3.9 gives us,

Equation 3.20

$$\mathbf{C}^2 \mathbf{A}_2^i = \begin{pmatrix} L_1(1-K)^i & \dots & L_1(1-K) & L_1 & L_1 \\ \vdots & \ddots & & \vdots & \vdots \\ L_n(1-K)^i & \dots & L_n(1-K)^i & L_n & L_n \\ (1-K)^i & \dots & (1-K)^i & 1 & 1 \end{pmatrix}$$

Again, by subtracting the last column from the second last column of the observability matrix, it follows that $\text{rank}(\mathbf{O}) \leq n+1 < n+2$ and the system cannot be observable. In this case the rows of each matrix block $\mathbf{C}^2 \mathbf{A}_2^i$ of equation 3.19 are all linearly dependent. This follows by subtraction of a scaled value of a specific row, from all other rows of the block. Hence only one row of each block remains nonzero after this procedure. These $n+2$ nonzero equations can be selected to correspond to the last rows of the blocks of equation 3.20. They are then identical and it follows that

$$\text{rank}(\mathbf{O}) = \text{rank}\left(\left(\left(\mathbf{C}^2\right)^T \quad \dots \quad \left(\mathbf{C}^2\right)^T\right)^T\right) = \text{rank}(\mathbf{C}^2) = 1 < n+2.$$

The second choice of measurement matrix now appears to be a very poor one.

3.2.2.2 Elimination of $P^{E+N}(t)$ with an outer loop power control model

Since only the sum $P^{E+N} + P_N$ is observable one may ask if it is possible to eliminate one of $P^{E+N}(t)$ and P_N with mathematical modeling. As it turns out, this is not possible either and the reason for this is explained below:

a. State space models

In order to model a system with a mathematically eliminated quantity, the state vector is chosen as [9]:

$$\text{Equation 3.21} \quad \mathbf{x}(t) = \begin{pmatrix} P_1^{Code}(t) \\ \vdots \\ P_N^{Code}(t) \\ P_N(t) \end{pmatrix}$$

Hence $P^{E+N}(t)$ is not included in the state vector although it is unknown. It must instead be eliminated from the measurement equations by a mathematical model of some kind. Now, the only quantity that is available for modeling is the outer power control loop. Assuming that this loop is operating properly and that all quantities have settled, it follows that [9].

Equation 3.22

$$\begin{aligned} P^{Total}(t) &= \frac{1}{L_i(t)} P_i^{Code}(t) \Rightarrow nP^{Total}(t) = \sum_{i=1}^n \frac{1}{L_i(t)} P_i^{Code}(t) \\ \Rightarrow P^{Total}(t) &= \frac{1}{n} \sum_{i=1}^n \frac{1}{L_i} P_i^{Code}(t) \end{aligned}$$

By application of the total power equation, it follows that

$$\text{Equation 3.23} \quad P^{Total}(t) = \left(\sum_{i=1}^N L_i(t) \right) P^{Total}(t) + P^{E+N}(t) + P_N(t)$$

\Leftrightarrow

$$P^{E+N}(t) = \left(1 - \sum_{l=1}^N L_l(t) \right) P^{Total}(t) - P_N(t)$$

\Leftrightarrow

$$P^{E+N}(t) = \left(1 - \sum_{l=1}^N L_l(t)\right) \left(\frac{1}{n} \sum_{i=1}^n \frac{1}{L_i(t)} P_i^{Code}(t)\right) - P_N(t).$$

Unfortunately, when the measurement equation is written out, the following results

Equation 3.24

$$\begin{aligned} P_{Measurement}^{Total}(t) &= \sum_{i=1}^n P_i^{Code}(t) + P^{E+N}(t) + P_N(t) + e^{Total}(t) \\ &= \sum_{i=1}^n P_i^{Code}(t) + \left(1 - \sum_{l=1}^N L_l(t)\right) \left(\frac{1}{n} \sum_{i=1}^n \frac{1}{L_i(t)} P_i^{Code}(t)\right) - P_N(t) + P_N(t) + e^{Total}(t) \\ &= \sum_{i=1}^n P_i^{Code}(t) + \left(1 - \sum_{l=1}^N L_l(t)\right) \left(\frac{1}{n} \sum_{i=1}^n \frac{1}{L_i(t)} P_i^{Code}(t)\right) + e^{Total}(t). \end{aligned}$$

b. Observability Analysis

Obviously, $P_N(t)$, cancels out and becomes unobservable from measurements of the total power using this approach [10]. Noting that $P_N(t)$ does not appear in the code power measurement either, it must be concluded that $P_N(t)$ remains unobservable from the available measurements also after elimination of $P^{E+N}(t)$.

This is, again, natural since the power control model only relates the total power to the (controllable) code powers. Neither $P^{E+N}(t)$ nor $P_N(t)$ are controllable quantities and hence they remain impossible to observe from the available measurements also after inclusion of the outer power control loop model. The elimination of either of them is hence a pointless action. A formal analysis can also be undertaken. The result follows, noting that all **A** matrices are diagonal and that this time the **C** matrix has a zero last column. Hence also the observability matrix has a zero last column and its nulls pace contains the basis vector.

Equation 3.25

$$\begin{pmatrix} 0 \\ \vdots \\ 0 \\ 1 \end{pmatrix}.$$

3.3 SOLUTIONS FOR LOAD ESTIMATION

3.3.1 Solution for scale factor errors

In order to avoid problems with front end scale factor errors, a relative rise over thermal measurement in the digital receiver is studied. Fortunately, all powers forming the RTWP as shown in equation 3.4 are equally affected by scale factor error; this cancels the scale factor errors $\gamma(t)$ as shown below:

Equation 3.26

$$N_R(t) = N_R^{DigitalReceiver}(t) = \frac{P^{Total,DigitalReceiver}(t)}{P_N^{DigitalReceiver}} = \frac{\gamma(t)P^{Total,Antenna}(t)}{\gamma(t)P_N^{Antenna}}(t)$$

$$= \frac{\gamma(t)P^{Total,Antenna}(t)}{\gamma(t)P_N^{Antenna}} = N_R^{Antenna}(t)$$

Where $N_R^{DigitalReceiver}(t)$ is the measured noise rise at the digital receiver is, $P^{Total,DigitalReceiver}(t)$ is the total received wideband power at the digital receiver and $P_N^{DigitalReceiver}$ is the estimated thermal noise level at the digital receiver.

3.3.2 Solution for noise floor estimation

As explained in section 3.2.1.1 and 3.2.2.2, both the approaches that is, linear estimation of $P^{E+N}(t)$ and using the power control loop for the elimination of E+N, turn out to be infeasible. Therefore, thermal noise power floor is estimated as the minimum power value during a certain interval of time. A method known as Bayesian minimum estimation algorithm (explained in chapter 4) is used for the precise estimation of noise floor.

3.4 SUMMARY

This chapter has reviewed the importance of RoT. The problems encountered while estimation of load estimation are highlighted. The analysis showed that only the sum $P^{E+N} + P_N$ is observable from the available measurements. Since both quantities are positive with normally nonzero mean values, the conclusion is that any linear estimator that attempts to estimate the two quantities simultaneously from measurements of total wide band power and code power is doomed. It is also made clear that the approach where $P^{E+N}(t)$ or $P_N(t)$ are eliminated by an outer power control loop model, does not lead to observability. Hence the conclusion is that the best that can be hoped for is to estimate the sum $P^{E+N}(t) + P_N(t)$. Further processing on this estimate is then required to obtain an estimate of the thermal noise power floor.

CHAPTER FOUR

4 DETAILED DESCRIPTION OF THE CURRENT ALGORITHM

4.1 INTRODUCTION

The Rise over Thermal (RoT) is defined as the quotient of the total uplink power of the cell and the thermal noise floor power. The total uplink power (RTWP) is readily measured in the RBS every TTI (10 ms). The RoT estimation is dependent on the precise estimation of the thermal noise power floor. As it is formerly proved in the previous chapter that it is not possible to estimate the noise floor using the linear estimation techniques, therefore there is a need to estimate thermal noise by Bayesian conditional probability density function of the minimum estimated residual power. The one dimensional conditional pdf of RoT is the result of the estimated pdf of RTWP and estimated conditional pdf of the thermal noise floor.

The algorithm is divided into five main blocks. Block 0 is responsible for adjusting the level of measured RTWP by adding bias before being fed to other blocks. The second part of algorithm, Kalman filter (Block 1) gives the estimate of level adjusted RTWP. For discretizing the power distribution, power grids are to be defined which is done on the prior histogram block (Block 2). Noise floor estimation block (Block 3) computes the minimum estimate of noise floor using the sliding window technique. RoT computation block (Block 4) will calculate the RoT with the received RTWP estimate from Kalman filter and the noise floor estimate from block 3. All these calculations are done for each antenna branch and summation is done at the Enhanced-Scheduler (E-SC) to find the actual RoT of the cell. In this chapter the complete description of the implemented algorithm will be explained.

The chapter will start with the block diagram and will be followed by the functionality of each block.

4.2 BLOCK DIAGRAM OF ROT

The algorithm for RoT estimation is divided into five blocks, as outlined by Figure 4.1

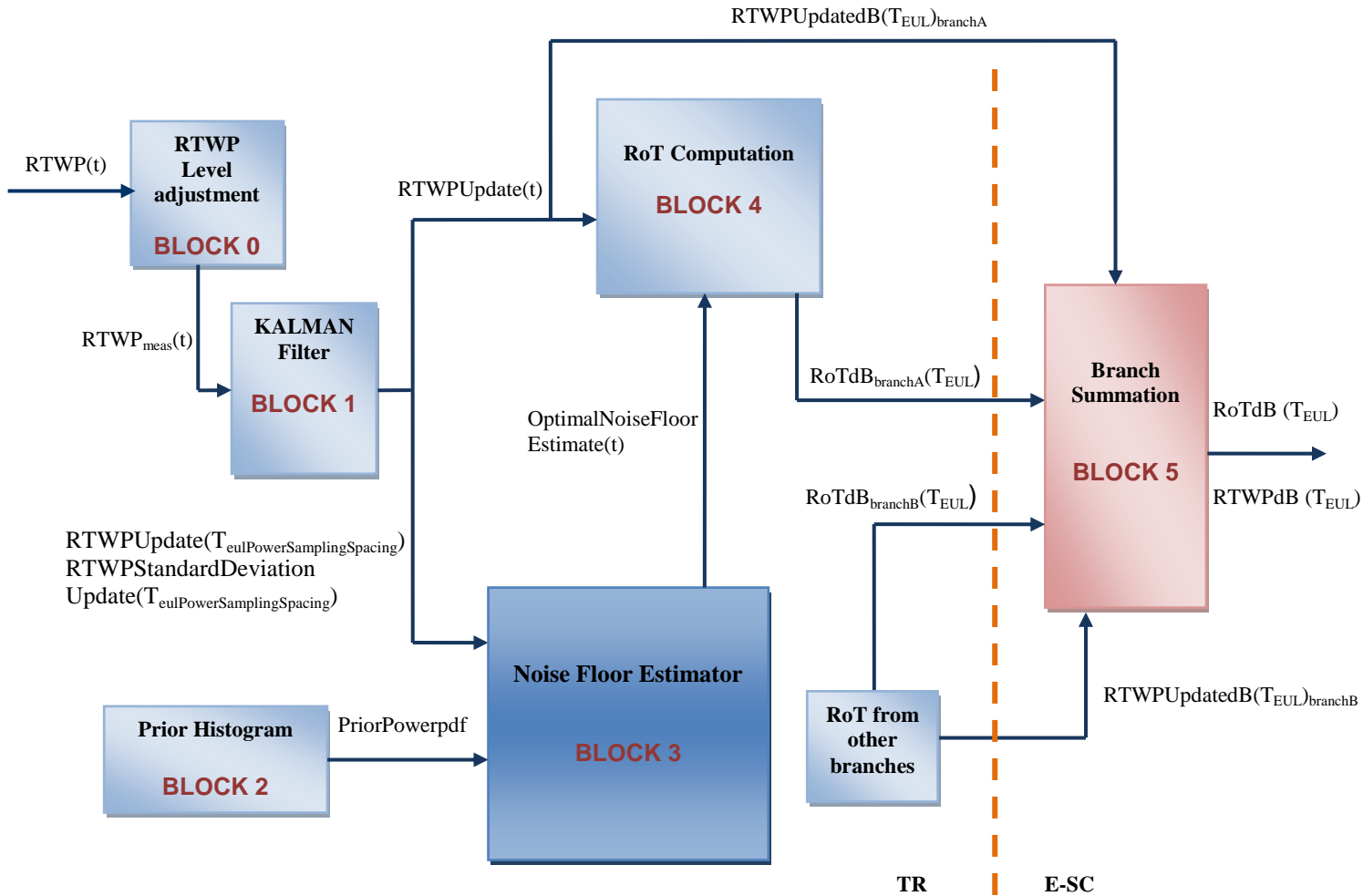


Figure 4.1 RoT Block diagram

A detailed description of each block and parameters involved is given below:

4.2.1 ALGORITHM BLOCK 0 – RTWP LEVEL ADJUSTMENT

The level of the RTWP is adjusted before it can be used for the later part of the algorithm. It takes care of the case that a RBS is configured in a way that the RTWP level is lower than the physically possible if the correct receiver gain figure were used. This is accomplished by detecting the low level and then compensating all used RTWP values with the same compensation. The detection is only done once when EUL is configured. A new setup of EUL in the cell causes a new detection attempt.

Description of the parameters being used in the block 0 is given below

Table 4.1

Parameter name	Description	Type	Unit
<i>eulThermalLevelPrior</i>	Level of the anticipated noise. It is the (power) centre of the distribution of the prior information for the thermal noise power level of the RBS. The other parameters related to the discretization grid of the noise power relate to this level in a relative manner. The advantage is that then the algorithm can be adjusted to different levels, by the modification of one single parameter.	Operator parameter	<i>dBm</i>
<i>eulSafetyNet1Margin</i>	The number of dB's below <i>eulThermalLevelPrior</i> that is used as noise floor is at start-up.	System constant	<i>dB</i>

Table 4.2

Variable name	Description	Unit
<i>rtwpThreshold</i>	A threshold below <i>eulThermalLevelPrior</i> under which the bias shall be triggered.	<i>dB</i>
<i>triggered</i>	A Boolean that is set to false initially, and is changed to true if the bias should be used	-
<i>bias</i>	A bias that is calculated once, when the condition is triggered, and then used to all RTWP measurements.	-
<i>triggerCounter</i>	A counter for how many times the RTWP measurement has been below the threshold	-
<i>RTWP_{meas}(t)</i>	Measured received total wideband power every 10ms	<i>dBm</i>

The $RTWP_{meas}(t)$ is measured every 10ms and depending upon the trigger counter that is if the measured value of RTWP is less then the first condition as given in the flow chart 4.1 for at least 100 times, the bias is added to the measured value of the RTWP.

Algorithm

This algorithm should be executed for each RTWP measurement:

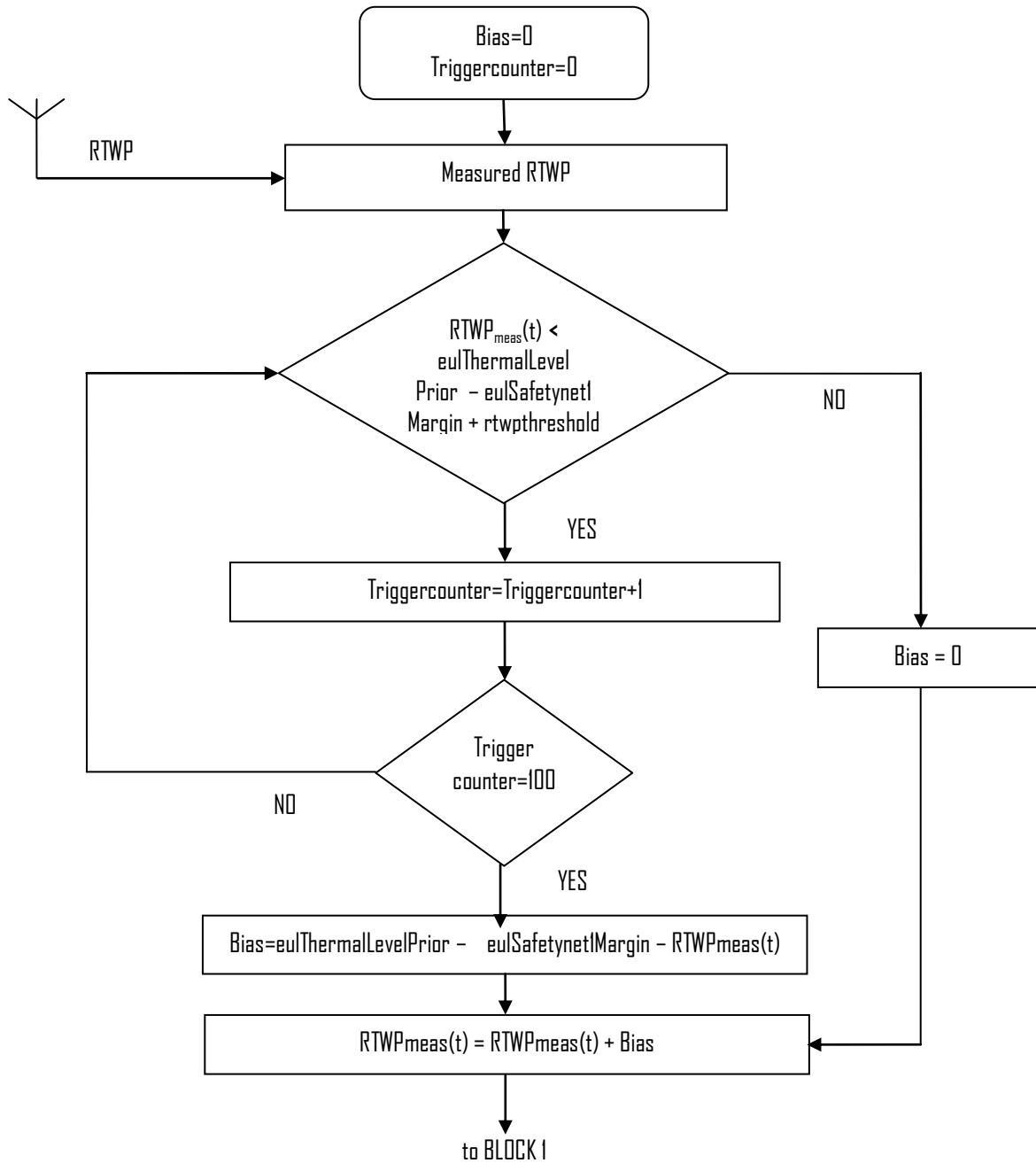


Figure 4.2 Flow Chart - Level Adjustment Algorithm

4.2.2 ALGORITHM BLOCK 1 – KALMAN FILTER

The second part of the RoT measurement algorithm is a Kalman Filter which produces an estimate of the distribution of RTWP received from Block 0. The main purpose of the Kalman filter is to find the variance

and the initial prediction of the RTWP using the random walk model. A time varying Kalman filter is used for this purpose. The estimation of the momentary total power needs to operate more or less close to TTI rate which is 10ms.

The Kalman filter operations are divided into three steps:

1. Transformation of parameters
2. Initialization
3. Estimation of RTWP

1. Transformation of Parameters

The first step is to transform the given parameters from logarithmic to linear domain using the following equation [12]:

Equation 4.1

$$\begin{aligned} \text{varianceRTWPSystemsNoiseLinear} &= 10^{-6} \cdot 10^{((\text{eulThermaLevelPrior} + \text{sigmaRTWPSystemsNoise}) / 5)} \\ \text{varianceRTWPMeasurementNoiseLinear} &= 10^{-6} \cdot 10^{((\text{eulThermaLevelPrior} + \text{sigmaRTWPMeasurmenNoise}) / 5)} \\ \text{initialRTWPPredictionLinear} &= 10^{-3} \cdot 10^{((\text{eulThermaLevelPrior} + \text{initialRTWPPrediction}) / 5)} \\ \text{initialRTWPVariancePredictionLinear} &= 10^{-6} \cdot 10^{((\text{eulThermaLevelPrior} + \text{initialRTWPSstandardDeviationPrediction}) / 10)} \end{aligned}$$

The description of these parameters is given in the table below:

Table 4.3

Parameter Name	Description	Unit
<i>sigmaRTWPSystemNoise</i>	The relative standard deviation of the systems noise of the RTWP random walk model	dB
<i>sigmaRTWPMeasurementNoise</i>	The relative standard deviation of the measurement noise of the RTWP measurement model	dB
<i>intialRtwpPrediction</i>	The relative initial value for the Kalman (prediction) of the estimated RTWP	dB
<i>initialRtwpStandardDeviationPrediction</i>	The square root of the relative initial value of the estimated Kalman (prediction) covariance	dB
<i>eulPowerSamplingSpacing</i>	The spacing between RTWP samples used for evaluation of minimum thermal level during the sliding window time. Set per cell.	sec
<i>varianceRTWPSystemNoiseLinear</i>	Absolute linear systems noise variance of the RTWP random walk model	W ²
<i>varianceRTWPMeasurementNoiseLinear</i>	Absolute linear measurement noise variance of the RTWP random walk model	W ²

<i>initialRtwPredictionLinear</i>	Absolute linear initial value for the Kalman (prediction) of the estimated RTWP	W
<i>initialRtwVariancePredictionLinear</i>	Absolute linear initial value of the estimated Kalman (prediction) covariance	W^2

2. Initialization

The Kalman Filter is initiated as shown in the following equation 2:

Equation 4.2

$$RTWPPrediction = initialRtw pPredictionLinear$$

$$RTWPVariancePrediction = initialRtw pVariancePrediction$$

The description of these quantities is given in the table below:

Table 4.4

Parameter Name	Description	Unit
<i>RTWPPrediction</i>	Prediction of RTWP provided by the Kalman filter	W
<i>RTWPVariancePrediction</i>	Variance of the predicted RTWP provided by the Kalman filter	W^2

3. Estimation of RTWP

The final step follows the basic Kalman filter iterations, that is; to find the Kalman gain, variance and the standard deviation which will be used to find the RTWP update and RTWP standard deviation update which will be used in the later part of the algorithm. Once the cell is configured with EUL, the Kalman iterations are repeated with a sampling period of T_{EUL} . Following equation illustrate these iterations [12]:

Equation 4.3

$$RTWPLinear = 10^{-3} 10^{(RTWP_{meas}(t)/10)}$$

$$KalmanGain = \frac{RTWPVariancePrediction}{RTWPVariancePrediction + varianceRTWPMeasurementNoiseLinear}$$

$$RTWPUdate = RTWPPrediction + KalmanGain \times (RTWPLinear - RTWPPrediction)$$

$$RTWPVarianceUpdate = RTWPVariancePrediction$$

$$- \frac{(RTWPVariancePrediction)^2}{RTWPVariance Prediction + varianceRTWPMeasurementNoiseLinear}$$

$$RTWPPrediction = RTWPUpdate .$$

$$RTWPVariancePrediction = RTWPVarianceUpdate + varianceRTWPSystemsNoiseLinear .$$

$$RTWPStandardDeviationUpdate = \sqrt{RTWPVarianceUpdate} .$$

Table 4.5

Variable Name	Description	Unit
$RTWP_{meas}(t)$	Measured RTWP value each T_{EUL}	<i>dBm</i>
$RTWPLinear(t)$	Measured RTWP value	<i>W</i>
$KalmanGain(t)$	Time variable gain, that is the update gain of the recursive filter	-
$RTWPUpdate(t)$	Updated RTWP estimate, that is the output of the filtering process	<i>W</i>
$RTWPVarianceUpdate(t)$	Variance of the updated RTWP estimate	W^2
$RTWPStandardDeviationUpdate(t)$	Square root of the variance of the updated RTWP estimate	<i>W</i>

A simple view of input, output quantities and the processes going on inside Kalman filter each TTI is illustrated in the figure below:

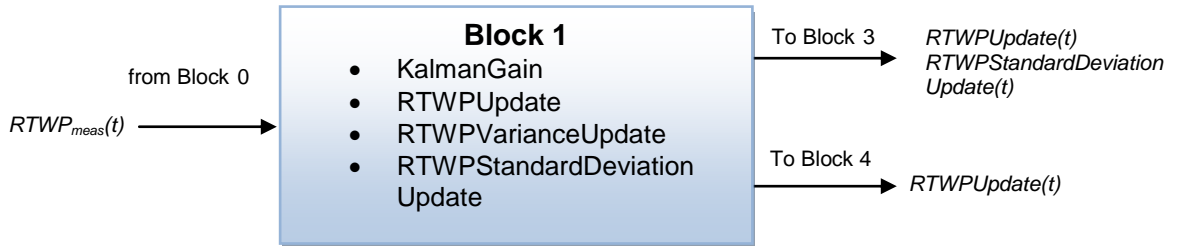


Figure 4.3 Kalman Filter

The rate with which the Kalman output is fed to second and third block is different. It can be clearly seen from the above figure that the output from the Kalman filter is *RTWP Update* and *RTWP Standard Deviation Update* are fed to block 3 and only *RTWP Update* is fed to block 4 with a rate of $(eulPowerSamplingSpacing)^{-1}$ and $(T_{EUL})^{-1}$ respectively.

4.2.3 ALGORITHM BLOCK 2 – PRIOR HISTOGRAM

At startup of the noise power floor estimation algorithm, the first step is to define the power grid on which all power distributions are to be discretized and to create the normalized prior power PDF.

Prior power PDF is the computed prior information of normalized distribution of the thermal noise level in dBm.

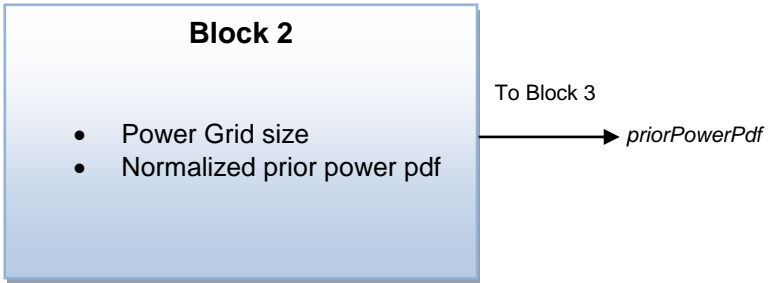


Figure 4.4 Prior Block

4.2.4 ALGORITHM BLOCK 3 – SOFT NOISE FLOOR ESTIMATOR

The main part of the RoT algorithm is the Noise Floor estimation block. The main task of this block is to create the Gaussian discretized probability distribution or the histograms of the power samples received from the Kalman Filter and use the sliding window to find the minimum estimate of noise floor [12]. An illustration of the Noise Floor Estimator block focusing on the input parameters and processing involved inside the block is given below:

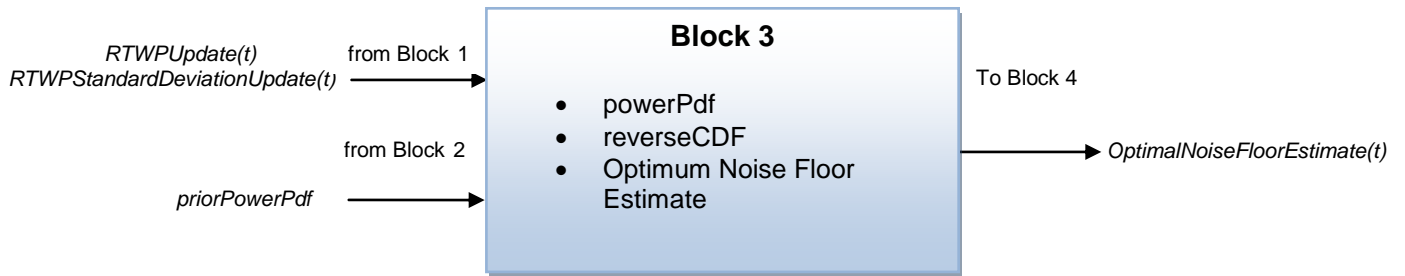


Figure 4.5 Noise Floor Estimator

The description of the parameters in the figure is given below:

Table 4.7

Parameter Name	Description	Type	Unit
<i>eulSlidingWindowTime</i>	The length of the sliding window during which a thermal noise level is found. Set per cell.	Operator controlled	sec
<i>slidingWindowSize</i>	Size of the sliding window used for noise floor estimation. It is an integer value obtained by rounding the floating point argument downwards to the nearest lower integer.	-	-

Functional Description

With $(eulPowerSamplingSpacing)^{-1}$ Hz a new RTWP estimate and a corresponding standard deviation arrives from the block 1 of the RoT estimation algorithm, as can be seen from above figure. For each such time instance, the remaining steps of this subsection are repeated.

Block 3 algorithm involves following steps:

1. **Definition of parameters**
2. **Calculation of power PDF**
3. **Calculation of reverse power CDF**
4. **Computation of Test Quantity**
5. **Detection algorithm**
6. **Calculation of optimal noise power floor**

1. Definition of Parameters

Before moving into the detailed algorithm of noise floor estimation, few preliminary steps are important to mention here:

The power and corresponding standard deviation samples collected from the sliding window that are the basis for the present estimate of noise floor power level are:

- *currentNumberOfSamples*
- *RTWPUpdate*
- *RTWPStandardDeviationUpdate*

$$slidingWindowSize = \text{floor} \left(\frac{eulSlidingWindowTime}{eulPowerSamplingSpacing} \right)$$

The division with ***eulPowerSamplingSpacing*** above must result in an integer. ***eulSlidingWindowTime*** and ***eulPowerSamplingSpacing*** should be jointly set, so that the number of samples in the sliding window is correctly optimized.

1. Calculation of Power PDF

After defining the parameters, the next step is to create the histograms or the discretized probability distribution of the received power samples. As the samples are Gaussian, the power PDF can be calculated by the following equation [13]:

Equation 4.6

$$f(x; \mu, \sigma^2) = \frac{1}{\sigma\sqrt{2\pi}} e^{-\frac{1}{2}\left(\frac{x-\mu}{\sigma}\right)^2}$$

Where σ is the RTWP Standard Deviation Update, μ is the RTWP Update and x is the power grid size as defined in the prior histogram (Block 2).

The **powerPDF** as given by the equation 4.6 is the discretized probability distribution of one estimate of **RTWP**.

2. Calculation of reverse Power CDF

The cumulative probability distribution (CDF) is defined as the integral of probability density function (PDF). The algorithm calculates the discretized conditional probability distribution of the minimum power (RTWP), conditioned on *powerPDF* calculated above and *priorPowerPDF* as defined by block 2. Instead of implementing the calculations as CDF, it is more efficient to implement them in terms of the reversed CDF function which is given by:

Equation 4.7

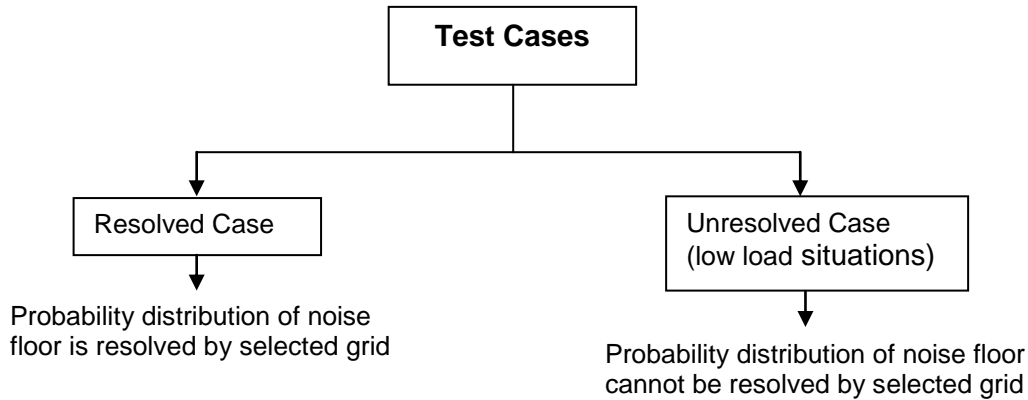
$$revPowerCdf = 1 - powerCDF$$

For direct computation of reverse power CDF the function $h(x) = 1 - \frac{1}{2}erfc(-x)$ is used. The complementary error function is given by [13]:

$$erfc(x) = \frac{2}{\sqrt{\pi}} \int_x^{\infty} \exp(-t^2) dt$$

3. Computation of Test Quantity

Two cases need to be treated when the thermal noise power floor is estimated. The first case is defined by a situation where the probability distribution of the thermal noise floor cannot be resolved by the selected grid (this may happen in low load situations). The other case is defined by a situation where the probability distribution of the thermal noise floor is resolved by the selected grid and where the soft thermal noise floor estimator can be applied as derived.



The algorithm first determines which case that applies by analysis of a test quantity.

CDFTest is a test quantity, used in order to check for the unresolved case and to calculate the thermal noise power floor in case the grid does not resolve the probability density function.

4. Detection Algorithm

The detection algorithm then proceeds by detecting the case where the test quantity falls from 1 to 0 when the power grid increases one step.

The algorithm determines if an unresolved or a resolved calculation of the thermal noise floor shall be performed. This is done by defining the detection flag i.e unresolvedCDF 1 or 0.

The algorithm determines if an unresolved or a resolved calculation of the thermal noise floor shall be performed. In case $unresolvedCDF = 1$ the algorithm proceeds with the unresolved case, otherwise the algorithm proceeds with the resolved case.

5. Calculation of optimal noise power floor

The last step is to find the optimal noise power floor by converting the un-normalized power pdf to normalized power pdf. Minimum Power PDF is the discretized conditional probability density function for the minimum power which helps to compute the optimal estimate of the minimum power, this estimate being the conditional mean. Optimal Noise Floor Estimate is the estimated value of the thermal noise power floor [12]. This optimal noise floor estimate is given as an input to block 4.

4.2.5 ALGORITHM BLOCK 4 – RoT COMPUTATION

An illustration of the Noise Floor Estimator block focusing on the input parameters is given below. RoT for each branch is calculated by simply dividing the two input parameters (estimates received from the corresponding branche).

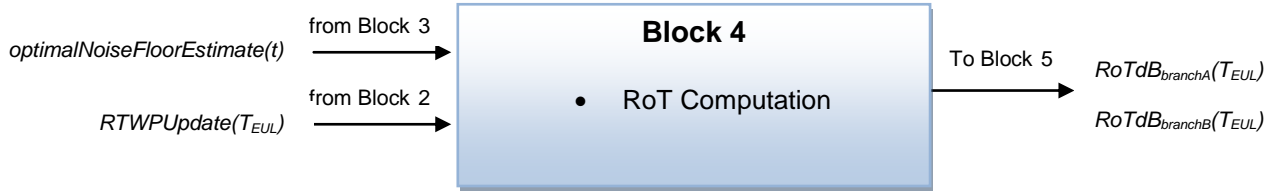


Figure 4.6 RoT Computation Block

4.2.6 ALGORITHM BLOCK 5 – BRANCH SUMMATION

Since the RoT measurement values are delivered to the ESC per branch, the branches allocated to the same cell has to be added together to form a value for the cell. It is done according to the following equation:

$$RoTEstimate_{cell}(t) = \frac{\sum_{n=1}^b 10^{(RoTEstimatedB_{branchn}(t) / 10)}}{no\ of\ cellbranches}$$

Where b is the number of cell branches

This ends the calculation of RoT.

CHAPTER FIVE

5 PROPOSED OPTIMIZED SOLUTION OF THE ALGORITHM

5.1 BLOCKWISE ANALYSIS OF THE CURRENT ALGORITHM

The estimation of RoT involves several steps which are described in detail in the previous chapter. In order to provide the possible solutions to reduce the complexity of the algorithm, block wise analysis will be made in this chapter. The Block diagram figure 4.1 consists of 5 blocks named the level adjustment block 0, Kalman Filter block 1, prior histogram block 2, noise floor estimator block 3 and the RoT computation block 5. Out of them the block 0 adjusts the level of the received power; block 2 defines the power grid on which the power distributions are to be discretized. This is used in the later part of the algorithm which is the preliminary step for the estimation of noise floor. RoT computation block 4 just involves the division of RTWP and the noise floor estimate from block 3. These three blocks (Block 0, 2 and 4) will not be discussed further in this chapter. However, the main focus would be on Kalman filter block 1 and noise floor estimator block 3 reason being most of the calculations are involved in these blocks. A critical analysis is performed based on two parameters which are:

- *Calculations involved in each block*
- *Update rate of each block*

In the coming sections, both these parameters will be discussed based on which it will be figured out what could be done either to simplify the calculations or to play with the update rate, thereby reducing the processor load.

5.1.1 Kalman Filter – Block 1

A time varying Kalman filter is used for the estimation of the measured value of RTWP received from block 0 and produces the Gaussian power pdfs.

5.1.1.1 Calculations involved

Kalman filter involves the basic iterations which are highlighted briefly below (as explained in detail in section 4.1.2):

- To find the time variable Kalman gain which is the update gain of the recursive filter.
- To provide RTWP Update which is the updated RTWP estimate using the Kalman gain.
- To provide the RTWP Standard Deviation update which is used in the block 3 (noise floor estimator) of the algorithm.

5.1.1.2 Update Rate of Block 0

The two outputs from the Kalman filter are the RTWP Update and RTWP Standard Deviation Update. It is clear from the figure 4.1 that only RTWP Update is required for block 4, however, both the outputs are required as input to block 3.

A point of interest here is that, the update rate for both these blocks is different, that is for RoT calculation (block 4) the values have to be updated each T_{EUL} (10ms) and for the noise floor estimation (block3) the values have to be updated each $T_{eulPowerSamplingSpacing}$ (30sec).

5.1.2 Noise Floor Estimator – Block 3

The most important part of the algorithm which involves the maximum number of calculations is the noise floor estimator block. A non-linear technique for minimum estimation, Bayesian probabilistic approach is used (as explained in section 4.1.4).

5.1.2.1 Calculations Involved

The noise floor estimator block calculates the following quantities each TTI that is, 10ms.

- Power PDF
- Reverse power CDF
- Test Quantity
- Detection Algorithm
- Optimal noise floor estimate

Power PDF making use of the RTWP Update and RTWP Standard Deviation Update from block 1 (the Kalman Filter), the discretized probability distribution, or the histograms, of the power samples are created. Since the samples are Gaussian, the distribution for finding the power PDF is given by,

Equation 5.1

$$f(x; \mu, \sigma^2) = \frac{1}{\sigma\sqrt{2\pi}} e^{-\frac{1}{2}\left(\frac{x-\mu}{\sigma}\right)^2}$$

Where μ is the mean or expectation and σ is the standard deviation. From equation 4.6 it can be seen that σ is the RTWP Standard Deviation Update and μ is the RTWP Update received from block 1. These pdfs (each sample) are discretized on a power grid size of 250 as defined by block 2 (prior histogram). Power PDF as given by the equation 4.6 is the discretized probability distribution of one estimate of RTWP.

Note: *The calculations performed here include floating point arithmetic.*

The expression of Power PDF involves the calculation of exponential which includes the floating point numbers and turns out to be quite complex especially when it is calculated each TTI.

Reverse Power CDF The algorithm then proceeds with the calculation of discretized conditional probability distribution of the minimum power, conditioned on power PDF equation 4.6 and prior power PDF equation 4.5. Cumulative probability density function is the integral of probability density function. The efficient way of implementing the calculations is in terms of reversed cumulative probability function. The reversed CDF is given by:

$$revPowerCDF = 1 - PowerCDF$$

The complementary error function used here to calculate the Power CDF is given as:

$$erfc(x) = \frac{2}{\sqrt{\pi}} \int_x^{\infty} \exp(-t^2) dt$$

Equation 4.7 gives a detailed expression used for the calculation of reverse power CDF. The function is implemented by linear interpolation in a table of double precision function values, reason being that it can be used for direct computation of reverse power CDF.

5.1.2.2 Update rate of Block 3

According to the current algorithm, the noise floor estimator block need not to be updated every TTI, instead is updated every *eulPowerSamplingSpacing* which is 30 seconds. However, all the calculations are being performed in one TTI, which leads to a peak processor load. The point of interest here is that, if the update of noise floor is not time critical then there could be a possibility of spreading the calculations over several TTIs which will smear down the peak. This will be discussed further in section 5.2.1.

5.2 PROPOSED SOLUTION FOR OPTIMIZATION

Without any hardware modification and by keeping the same software interface, some possibilities for reducing the processor load have been proposed. The proposed solution is recommended for both cases, that is; for reducing the peak processor load and average processor load. Figure 5.1 is the proposed block diagram for RoT Algorithm with slight modifications to the current block diagram. The level adjusted RTWP from block 0 is directly fed to RoT computation block (block 4). The Kalman filter is updated on quite lower rate i.e.; only when it's necessary for the noise floor estimation block (Block 3) This helps for the reduction of average load, as Kalman filter is not updated every TTI. The calculations within the Block 3 are calculated in 4 TTIs, with slight modification in the computation. Rest of the algorithm blocks operates in the similar way as in the current algorithm. Details are given in the coming sections.

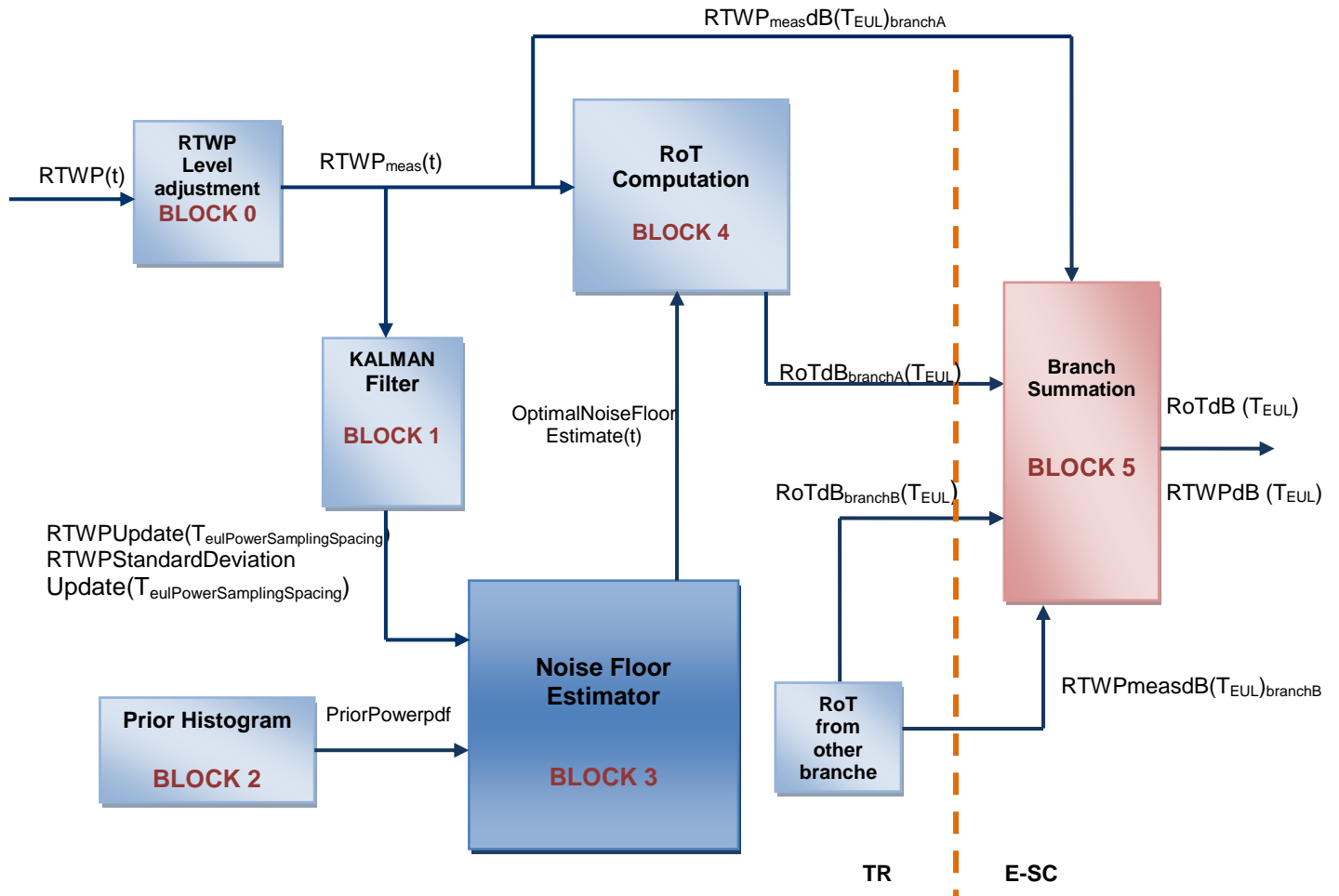


Figure 5.1 Proposed Block Diagram

5.2.1 Methods to Reduce Processor Load

There could be two ways to reduce the processor load as explained below:

1. Reduction of peak processor load
 - a. Tabulation of the exponential function (Equation 4.6)
 - b. Spreading of the calculation in several TTIs'
2. Reduction of the average processor load
 - a. Change the update rate of Block 1 i.e.; Kalman Filter.

5.2.1.1 Reduction of Peak Load

a. Tabulation of the exponential function

As described in the section 5.1.2.1, the calculations of power PDF for estimation of thermal noise power, involves the transcendental floating point operations. The processors in Platform 4 does not have any hardware support for floating point and mathematical functions. Therefore, there is a need to find some other way for the calculation of exponential which can bring down the processor load to some extent. For this purpose the exponential function was tabulated for the range which is enough to cover all the possible power levels. The table has two rows, first row of the table has the vectors ranging from -32.5 to 0 and in the second row comprises of the corresponding values of exponential. Linear interpolation is used to calculate exponential by fetching the value of the calculated argument of the exponential function of equation 4.6, from the table of size 77 KB stored in the memory, instead of direct calculation. A range of -32.5 till 0 is covered with a spacing of 0.01. If the argument lies outside this range the power PDF is set to zero for those points.

This helps to avoid the complex calculation involved for finding the exponential of floating point numbers, which will ease the processor.

The analysis of the modified algorithm is made on the basis of two parameters:

- Operations and Instruction Count
- Performance Loss

The operations and Instruction count analysis is made using the User Manual of the processor core used in Platform 4. Although the timing descriptions do not provide the complete description of the performance but it gives a good representation of number of cycles if there is no wait for the memory access. All the instructions execute in one clock cycle except the divide instruction which takes 35 clock cycles to execute and the multiply instruction uses 4 clock cycles. The approximate number of clock cycles (hand calculation) for instructions and operations are listed below:

Analysis

The analysis is made based on the number of arithmetic operation count involved in the calculation of exponential. Table 5.1 shows the number of additions, multiplications, subtractions, divisions, square root, carried out for the calculation of PDF.

Arithmetic Operations/ Instructions	Without Tabulation		With Tabulation	
	Count	Clock cycles	Count	Clock cycles
Multiplications	115	115x4=460	43	43x4=172
Subtractions	23	23x1=23	21	21x1=21
Additions	51	51x1=51	10	10x1=10
Square Root	11	11x1=11	10	10x1=10
Log	2	2x1=2	-	-
Memory Fetch	-	-	60	60x1=60
Divisions	41	41x35=1435	21	21x35=735
Total	243	1982	165	1008

Table 5.1: Comparison of Clock Cycles with and without Tabulation of exponential function

As it can be seen from the above table that there is a significant decrease in the cycle count when then tabulation is used, instead of direct computation.

Simulation Results:

The simulations were performed in MATLAB, using the different set of power levels, and it was observed that by making the above changes, there is no significant performance loss in the estimation of RoT. Figure 5.1 shows the RoT before Tabulation and the figure 5.2 shows the RoT after tabulation.

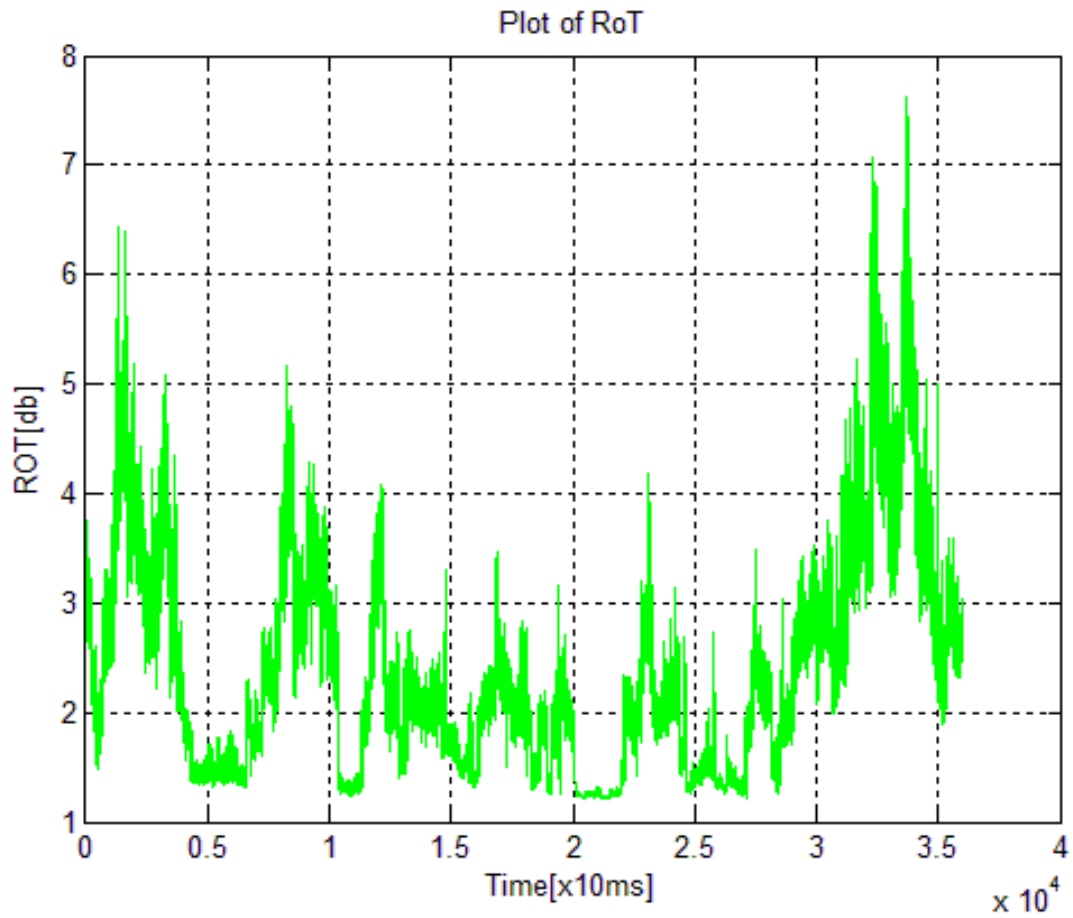


Figure 5.2 RoT (Without Tabulation)

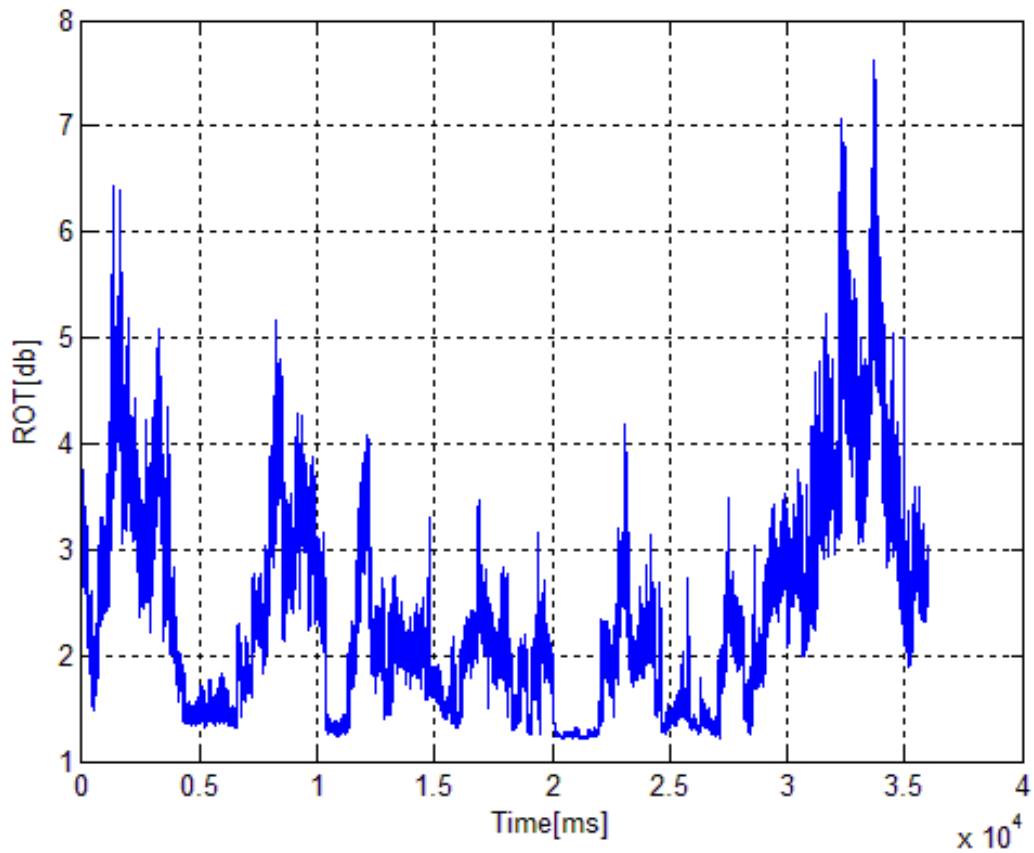


Figure 5.3 RoT (with tabulation)

It can be seen that, by reducing the number of clock cycles, the processor load can be reduced without any performance loss.

b. Distributing the calculation of Noise Floor estimate in four TTI's

Noise floor estimation block involves several mathematical calculations, as explained in detail in Chapter 4, within a single TTI which is 10ms. It requires the calculation of Power PDF, reverse Power CDF, CDF Test, detection algorithm, and finally optimal noise floor estimation. As explained in section 5.1.2.2, the update rate of Noise Floor estimator block is 30 seconds, whereas the other blocks require more frequent update rate of 10ms. Based on this, the parameters which are calculated in this block can be divided into several TTI's so that the work load within a single TTI will be reduced. The splitting is done as follows:

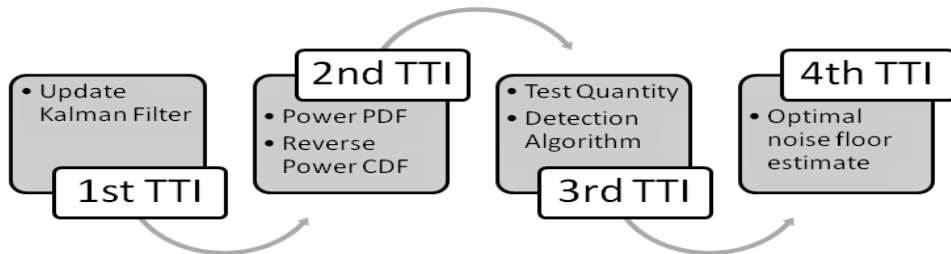


Figure 5.4 Calculations involved in Noise Floor Estimation

The Kalman Filter is updated in the first TTI, second TTI calculates the power PDF and reverse power CDF, test quantity and detection algorithm applies in third TTI and finally the optimal noise floor estimate is calculated in fourth TTI. The pseudo code is attached as Appendix B.

Analysis

The number of operations involved in the calculation of optimal noise floor estimate is listed in the table below. Instead of performing this in one TTI if these calculations are spread as proposed above they will reduce the clock cycles involved for a single TTI and hence will reduce the peak load to a significant amount.

Arithmetic Operations/ Instructions	First TTI		Second TTI		Third TTI		Fourth TTI	
	Count	Clock Cycles	Count	Clock Cycles	Count	Clock Cycle	Count	Clock Cycle
Multiplication	40	160	54	216	131	524	115	460
Subtraction	2	2	52	52	1	1	110	110
Addition	12	12	30	30	10	10	200	200
Square root	1	1	11	11	-	-	-	-
Log	-	-	-	-	-	-	-	-
Memory Fetch	-	-	120	120	-	-	-	-
Division	14	490	42	1470	-	-	20	700
Initialization	-	-	-	-	708	708	250	250
Total	69	665	309	1899	850	1243	695	1720

Table 5.2: Clock cycle count for each TTI

Simulation Results:

After splitting the calculations over four TTIs it was observed that there was no effect on the final result that is the computation of RoT. All the parameters are calculated in the same way, like they were before (without optimization), the only difference being that the calculations which were performed in one TTI (which were responsible for the peak load) are now being performed over a wider range of time as shown in figure 5.4.

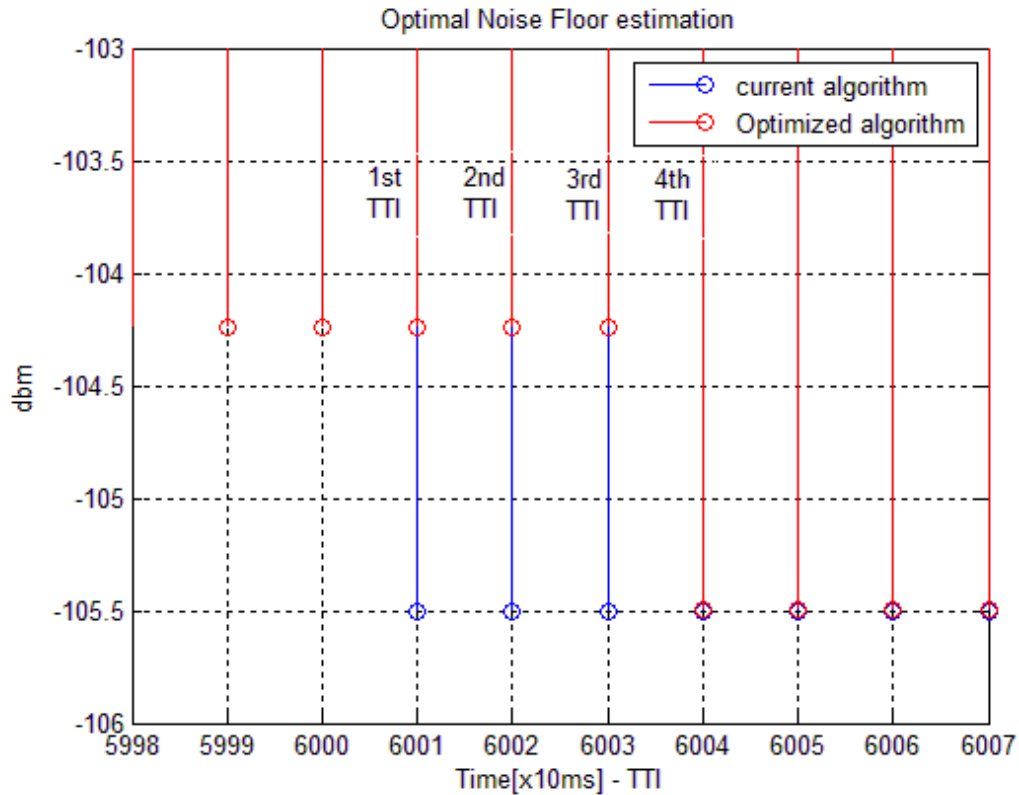


Figure 5.5 Update of Noise Floor in 4 TTIs

In the above figure the blue color shows noise floor calculated in the current algorithm. We observe the noise floor update of 105.5dbm and the same value is used till the next update of noise floor is required, which is 30 seconds. If we see the red line, it shows that a portion of the noise floor is calculated in first 10ms, the second in the next 10ms and so on. The final value of noise floor is updated at the fourth TTI. It can be clearly seen that, the noise floor which was calculated in 10ms previously, its now calculated in 40ms, thereby reducing the processor load.

5.2.1.2 Reduction of Average Load

Average load refers to the over all load on the processor, taking into account the processing load of each block involved in the computation of RoT. It can be seen from the block diagram 4.1 that the output of Kalman filter is RTWP Update and the RTWP Standard Deviation Update. However, only an estimate of RTWP which is fed to the block 4 required for the final result of the algorithm. After comparing the output from block 0 that is the level adjusted RTWP and the block 1 which is the estimated RTWP from Kalman filter, it was observed that there was no significant difference between these two outputs as can be seen in figure 5.5 that both the outputs are completely overlapping.

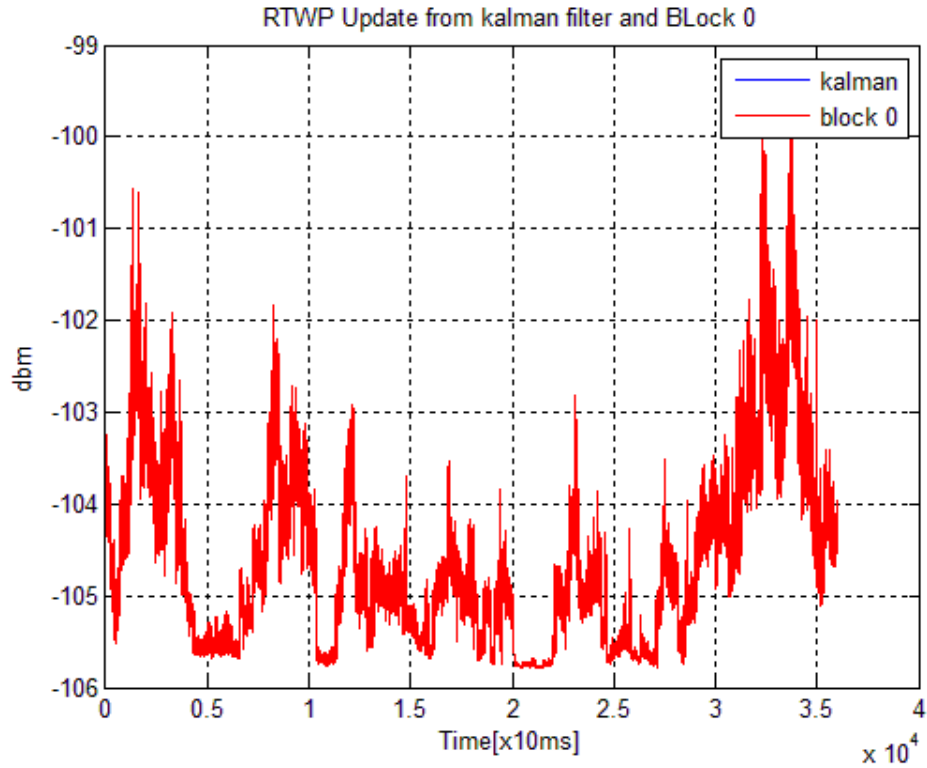


Figure 5.6 RTWP from Block 0 and Block 1 (Kalman filter)

Therefore the output was directly fed to the block 4 as shown in the proposed block diagram from block 0 and the Kalman filter was only updated when the noise floor update was required. This means that the update rate of Kalman filter will be 30 seconds instead of every 10ms, which will lead to a reduction of about 621 clock cycles (Table 5.2) each TTI.

The similar thing can be also represented by the figure 5.6 below that, previously the Kalman was updated every TTI (blue) but the red colour indicates the instances where the Kalman update is performed only when it required for the noise floor estimation.

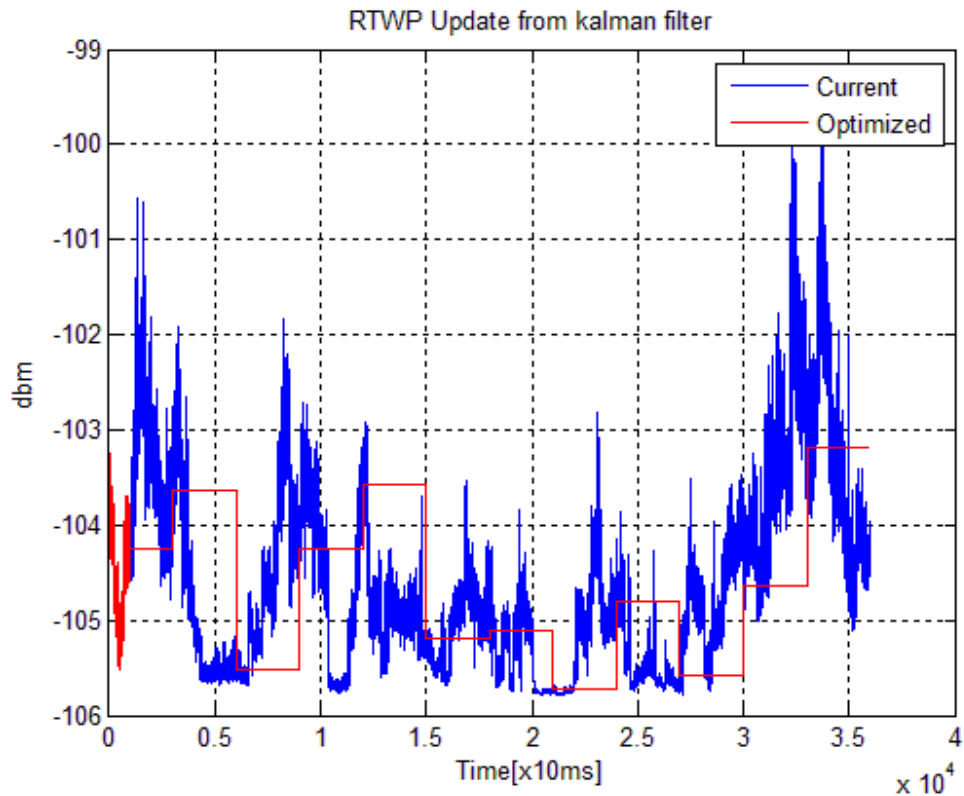


Figure 5.7 Update rate of Kalman Filter

5.3 SUMMARY

In this chapter the current RoT algorithm has been reviewed critically in order to reduce the complexity and to optimize it in terms of processing power. Two techniques to reduce the average and peak load have been discussed. The performance analysis have shown that, the proposed modifications lead to the considerable reduction in the clock cycles without any compromise on the over all performance of the algorithm.

CHAPTER SIX

6 CONCLUSIONS AND FURTHER WORK

This thesis work has mainly covered the detailed description of the implemented algorithm for the estimation of Rise-over-Thermal (RoT) used for the scheduling of Enhanced-Uplink (E-UL) channels. The basic block diagram used for this purpose has been explained in detail. Furthermore the analysis showed that certain steps of the algorithm can be circumvented in order to optimize the algorithm. For this, mainly three major changes are proposed in the current algorithm, two for the reduction of peak load and one for the reduction of average load. Chapter 5 has comprehensively covered these changes.

The first change proposed is to perform the transcendental calculations, involving floating point arithmetic, with the help of interpolation using a pre-stored table of 77 KB, instead of calculating it directly every time a new value of power arrives. The second change proposed for reducing the peak load is to spread the calculations over time. As it is mentioned in detail, the noise floor estimation in the algorithm comprises the calculation of power PDF and reverse power CDF, the Detection algorithm and finally the optimal noise floor estimate. All these parameters were being calculated in a single TTI that is, 10 ms. However, noise floor estimator is the only block in the algorithm which does not need to be updated every TTI. Instead, it is updated every 20 minutes. In view of this, the calculations mentioned above were spread over four TTIs which will result in smearing down the peak. The third change which is incorporated in the proposed block diagram is mainly for reducing the average load on the processor. For this, instead of using the estimated value of the received total wideband power RTWP for the computation of RoT, the level adjusted RTWP from block 0 is directly used. This has reduced the update rate of the first block which is the Kalman Filter block as well. Initially, Kalman filter was updated each TTI, but as per the proposed changes, it is updated only when its output is required for the noise floor estimator, which would be similar to the update rate of noise floor estimator block, that is every 20 minutes.

After making the above changes to the algorithm, the performance of the algorithm was investigated in order to check if the algorithm is still working as expected. Due to the limitation of resources, actual measurements could not be made on the target system. However, MATLAB simulations revealed that after making above changes there is no significant performance loss and the algorithm gives the same results as old one. Also, coarse hand calculations were made in order to compare the number of arithmetic operations of the old code and the optimized one. This was done using the hardware manual of the processor used in Platform 4, and number of cycles are counted needed per arithmetic operation. A significant decrease in the number of clock cycles was observed as mentioned in chapter 5.

It is important to mention here that the calculations made are hypothetical, there would be a variation when the algorithm is tested on the target system, but there would definitely be a decrease in the processor load. By implementing the proposed changes in the algorithm, the processor load can be reduced with a significant amount which will in turn save processing power. As, RoT is not the only algorithm running in Radio, optimizing this algorithm will increase the capacity of adding new features to the Radio.

The recommended future work as a result of this master thesis is to implement the proposed changes and to perform testing on the target system.

```
In main algorithm check the
if Noise Floor Estimation is required
{
    Update Kalman filter;
    innercounter==innercounter+1;
}
goto the main algorithm

if (innercounter==1)
{
    calculate PowerPDF;
    calculate RevPowerCDF;
    innercounter==innercounter+1;
}
goto the main algorithm

elseif (innercounter==2)
{
    calculate CDFTest;
    detection Algorithm;
    innercounter==innercounter+1;
}
goto the main algorithm

elseif (innercounter==3)
{
    find optimal Noise floor estimation;
    innercounter==0;
}
end

else goto the main algorithm

end

goto main algorithm
```


ABBREVIATIONS

3GPP	Third Generation Partnership Project
ARQ	Automatic Repeat Request
AUC	Authentication Center
BSS	Base Station Subsystem
CDF	Cumulative Distribution Function
CDMA	Code Division Multiple Access
CN	Core Network
CS	Circuit Switched
DCH	Dedicated Channel
EIR	Equipment Identity Register
E-DCH	Enhanced Dedicated Channel
E-DPDCH	Enhanced Dedicated Physical Data Channel
E-DPCCH	Enhanced Dedicated Physical Control Channel
ESC	Enhanced Scheduler
ETSI	European Telecommunication Standard Institute
E-UL	Enhanced Uplink
FDD	Frequency Division Duplex
G-GSN	Gateway GPRS Support Node
GMSC	Gateway Mobile Switching Center
GPRS	General Packet Radio Service
GSM	Global System for Mobile Communication
HLR	Home Location Register
HSDPA	High Speed Download Packet Access
HS-DPSCH	High Speed Physical Downlink Shared Channel
HS-DSCH	High Speed Downlink Shared Channel
HSUPA	High Speed Uplink Packet Access
IP	Internet Protocol
ISDN	Integrated Services Digital Network
MGW	Media Gateway
M-PBN	Mobile Packet Backbone Network
MSC	Mobile Switching Centre
PDF	Probability Density Function
PS	Packet Switched
PSTN	Public Switched Telephone Network
QAM	Quadrature Amplitude Modulation
QPSK	Quadrature Phase Shift Keying
RAN	Radio Access Network
RBS	Radio Base Station
RNC	Radio Network Controller

RoT	Rise over Thermal
RRM	Radio Resource Management
RTWP	Received Total Wideband Power
S-GSN	Service GPRS Support Node
SIR	Signal to interference ratio
TDD	Time Division Duplex
TTI	Transmission time interval
UE	User Equipment
UMTS	Universal Mobile Telecommunication System
USIM	Universal Subscriber Identity Module
UTRA	Universal Terrestrial Radio Access
UTRAN	UMTS Terrestrial Radio Access Network
VLR	Visitor Location Register
WCDMA	Wideband Code Division Multiple Access

References

- [1] E. Dahlman, S. Parkvall, J. Sköld, and P. Beming, 3G Evolution—HSPA and LTE for Mobile Broadband. Oxford, U.K.: Academic, 2007.
- [2] E.G. Lundin, F. Gunnarsson and F. Gustafsson, "Uplink load estimation in WCDMA", *Proc. IEEE Wireless Communication and Networking Conference*, New Orleans, LA, U.S.A, 2003.
- [3] M.R. Karim, M. Sarraf, W-CDMA and cdma2000 for 3G Mobile Networks. New York.: McGraw-Hill, 2002.
- [4] *Requirements for support of radio resource management (FDD)*, 3GPP TS 25.133, release 6 (v. 6.10.0), June, 2005. Available: <http://www.3gpp.org/ftp/Specs/html-info/25133.htm>.
- [5] H. Holma and A. Toskala, WCDMA for UMTS—Radio Access for Third Generation Mobile Communications. Chichester, U.K.: Wiley, 2000.
- [6] A. R. Mishra, Advanced Cellular Network Planning and Optimisation. Chichester, U.K.: Wiley, 2007
- [7] J. Zander, "Transmitter power control for co-channel interference management in cellular radio systems", in *Proc. WINLAB Workshop*, New Brunswick, NJ, 1993, pp. 241–247.
- [8] *FDD Enhanced Uplink; Overall description; Stage 2*, 3GPP TS 25.309, release 6 (v6.3.0), June, 2005. Available: <http://www.3gpp.org/ftp/Specs/html-info/25309.htm>.
- [9] T. Wigren, "Low Complexity Kalman Filtering for Inter-Cell Interference and Power Based Load Estimation in the WCDMA Uplink", in *Proc. 5th International Conference on Signal Processing and Communication Systems*, ICSPCS 2011, Honolulu, HI, December 12-14, 2011.
- [10] T. Wigren, "Soft uplink load estimation in WCDMA", *IEEE Trans. Vehicular Tech.*, June, 2007
- [11] T. Glad and L. Ljung, Reglerteknik – Grundläggande teori. Studentlitteratur, 1989.
- [12] T. Wigren and P. Hellqvist, "Estimation of uplink WCDMA load in a single RBS", *IEEE VTC2007-Fall*, Baltimore, MD, U.S.A., October 1-3, 2007.
- [13] T. Söderström, *Discrete-Time Stochastic Systems- Estimation and Control*. Hemel Hempstead, UK: Prentice Hall, 1994.